



การสร้างแบบจำลองสามมิติของชิ้นส่วนกระดูกสันหลังจากภาพถ่ายเอ็กซเรย์สองมิติ

Three-Dimensional Model of Vertebrae Bone Deformation from Bi-Plane X-Ray
Image

WATCHARAPHONG YOOWAN

Burapha University

2018

การสร้างแบบจำลองสามมิติของชิ้นส่วนกระดูกสันหลังจากภาพถ่ายเอ็กซเรย์สองมิติ



วัชรพงศ์ อยู่ขวัญ

วิทยานิพนธ์นี้เป็นส่วนหนึ่งของการศึกษาตามหลักสูตรวิทยาศาสตรมหาบัณฑิต

สาขาวิชาวิทยาการสารสนเทศ

คณะวิทยาการสารสนเทศ มหาวิทยาลัยบูรพา

2561

ลิขสิทธิ์ของมหาวิทยาลัยบูรพา

THREE-DIMENSIONAL MODEL OF VERTEBRAE BONE DEFORMATION
FROM BI-PLANE X-RAY IMAGE



WATCHARAPHONG YOOKWAN

A THESIS SUBMITTED IN PARTIAL FULFILLMENT OF
THE REQUIREMENTS FOR MASTER OF SCIENCE
IN INFORMATICS
FACULTY OF INFORMATICS
BURAPHA UNIVERSITY

2018

COPYRIGHT OF BURAPHA UNIVERSITY

The Thesis of Watcharaphong Yookwan has been approved by the examining committee to be partial fulfillment of the requirements for the Master of Science in Informatics of Burapha University

Advisory Committee

..... Principal advisor
(Assistant Professor Krisana Chinnasarn)

Examining Committee

..... Principal
examiner

(Assistant Professor Paramate Horkaew)

..... Member

(Assistant Professor Suwanna Rasmequan)

This Thesis has been approved by the Faculty of Informatics to be partial fulfillment of the requirements for the Master of Science in Informatics of Burapha University

..... Dean of the
Faculty of
Informatics
(Assistant Professor Krisana Chinnasarn)

59910233: MAJOR: INFORMATICS; M.Sc. (INFORMATICS)
KEYWORDS: DEFORMATION, VERTEBRAL BODY, LOW RADIATION,
TRIANGULAR ANALYSIS, THREE DIMENSION MODEL

WATCHARAPHONG YOOWAN : THREE-DIMENSIONAL MODEL OF
VERTEBRAE BONE DEFORMATION FROM BI-PLANE X-RAY IMAGE. ADVISORY
COMMITTEE: KRISANA CHINNASARN, Ph.D. 2018.

Three Dimension model of human spine become an important material in variety of medical routine. Many applications were proposed to reconstruct a 3D model of human spine. By using images form CT scanner or another High dose of X-ray machine, the model of human vertebrae is deformed. Dual-Energy X-ray Absorptiometry Scanner plays an important role in medical diagnosis and clinical routine. Typically, this kind of machine produces two radiography images of human spine consisted of Anteroposterior and Lateral side. However, these two images provided different viewpoints. Thus, in this proposed method consists of three main phase. Firstly, Region of interest of human lumbar spine is proposed. In the second phase, the vertebrae pose is identified for registration. In the final phase, the three dimensional model of human spine was deformed.

In the first phase, a method for segmenting region of interest on lumbar spine using a horizontal projection and geometric triangulation analysis is proposed. The proposed method offered an automated detection of lumbar spine that can reduce computational time and complexity in medical diagnosis. The result of the proposed method can help support many applications such as lumbar vertebrae pose segmentation, bone mineral density analysis and vertebral pose deform In the second phase, we proposed a method to automatically estimate human vertebrae pose in lateral-side image by using Multi-theta Orientation Gabor Filter combined with Principle Component Analysis and Geometric Ellipse Shape Analysis. The proposed method offered an automated estimation of human lumbar vertebrae pose that can reduce work load of radiologist, computational time and complexity in various bone-clinical applications. The result of the proposed method can help support many applications such as lumbar vertebrae pose segmentation, bone mineral density analysis and vertebral pose deformation. The proposed method can estimate the vertebrae pose with 86.4% for accuracy, 80.5% of recall, precision for 89.11% and 13.6% of false negative rate. In the final phase, the three-dimensional model template of human vertebrae is used to deform a model of human lumbar vertebrae from L1 to L4. The template file contains vertices and polygon-faces of lumbar shape in three-dimension space. Then, the surface of the model has been created. The result of this phase is evaluated by Mean Square Error of Volume compare with ground-truth. The L1 and L4 vertebral is gain a huge errors. Because of the information from vertebrae pose estimation step, L1 and L4 are located on a very low contrast area and disturbed with obstacles.

ACKNOWLEDGEMENTS

First of all, I would like to express my sincere gratitude to the National Research Council of Thailand (NRCT), fiscal year 2017 for providing me to pursue my master degree in Informatics.

Secondly, I would like to thank my advisor Assistant Professor Dr. Krisana Chinnasarn for assistance and wonderful guidance with this thesis.

Thirdly, I would like to express my special thanks to all lecturers especially Assistant Professor Dr. Paramate Horkeaw and Assistant Professor Dr. Suwanna Rasmequan for a great support in instructions and good advice.

Watcharaphong Yookwan

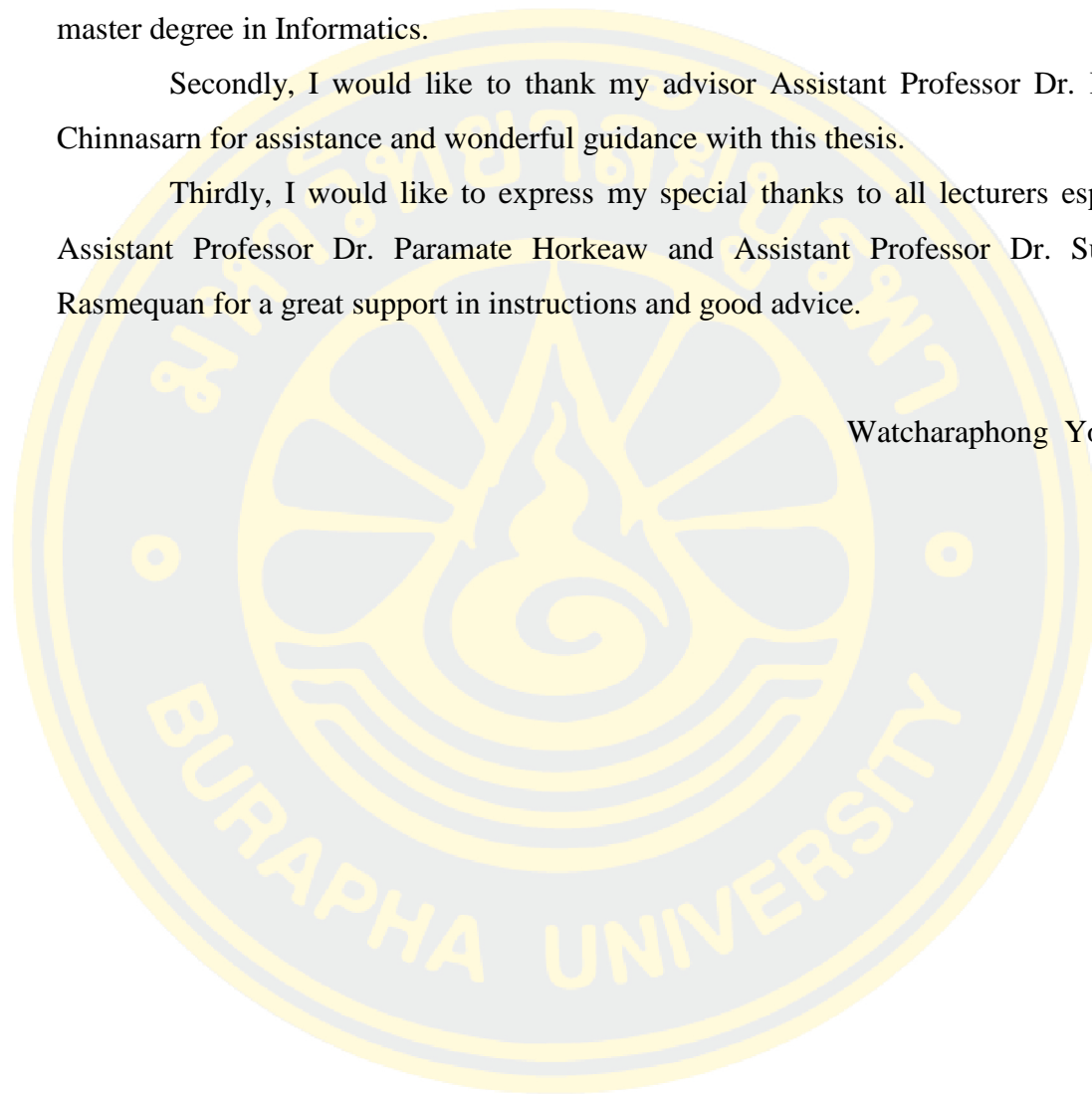
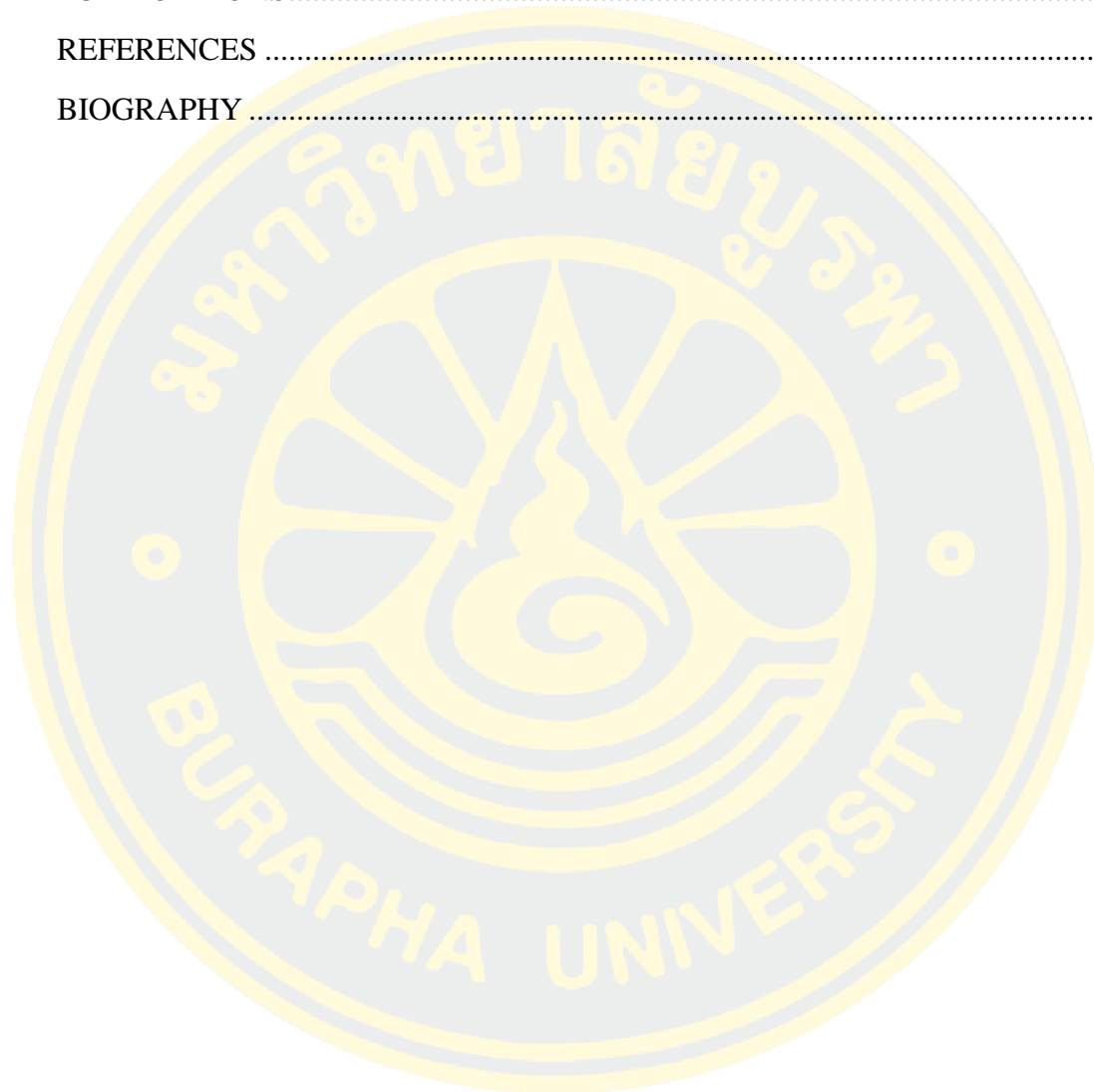


TABLE OF CONTENTS

	Page
ABSTRACT.....	D
ACKNOWLEDGEMENTS.....	E
TABLE OF CONTENTS.....	F
LIST OF TABLES.....	I
Table of Figure.....	J
CHAPTER 1.....	1
INTRODUCTION AND PROBLEM REVIEW.....	1
1.1 Introduction.....	1
1.2 Statements of the Problems.....	3
1.3 Research Objective.....	4
1.4 Scope of the Study.....	4
1.5 Research Advantage.....	4
1.6 Schedule plan.....	5
CHAPTER 2.....	6
THEORETICAL BACKGROUND.....	6
AND RELATED LITERATURE.....	6
2.1 Theoretical Background.....	6
2.1.1 Anatomy of the Spine.....	6
2.1.2 Low radiation image.....	8
2.1.3 Image Segmentation.....	8
2.1.4 Thresholding.....	9
2.1.5 Morphological Operation.....	10
2.1.7 Gabor Filter.....	12
2.1.8 Top-Hat Filtering.....	13
2.1.8 Connected Component Labelling.....	14

2.2 Literature Review	15
CHAPTER 3	27
METHODOLOGY	27
3.1 Region of Interest Identification	28
3.1.1 Binarization	28
3.1.2 Small objects removing.....	28
3.1.2 Horizontal Projection	29
3.1.2 Triangular Analysis.....	30
3.2 Vertebrae Pose Estimation.....	33
3.2.1 Image Enhancement using Top-Hat filter.....	33
3.2.2 Multi-theta Orientation Gabor Filter.....	34
3.2.3 Geometric-Ellipse Shape Analysis.....	36
3.2.4 Anterior-Posterior (AP) View lumbar vertebrae pose estimation.....	38
3.3 Three-dimensional Model Deformation	39
3.3.1 Registration	39
3.3.2 Deformation	40
CHAPTER 4	45
EXPERIMENTAL RESULTS.....	45
4.1 Region of Interest Segmentation	45
4.1.1 Binarization using Image Entropy value	45
4.1.2 Horizontal Projection	46
4.1.2 Triangular Analysis	47
4.2 Lateral Vertebrae Pose Estimation	52
4.3 Three-Dimensional Deformation.....	54
CHAPTER 5	58
CONCLUSION AND DISCUSSION	58
5.1 Conclusion	58
5.2 Contributions	59
5.3 Discussion.....	60

5.3 Future Work.....	60
APPENDIX.....	61
ETHICS.....	62
PUBLICATIONS.....	63
REFERENCES	77
BIOGRAPHY	79



LIST OF TABLES

	Page
Table 1 Work schedule plan in year 2017	5
Table 2 Percentage of Jaccard index and AO	49
Table 3 Conclusion of percentage of Jaccard index and Area Overlap.....	50
Table 4 Percentage of True Positive (TP), False Negative (FN), False Positive (FP), and True Negative (TP) using Eduardo A. Ribeiro's method.	51
Table 5 Percentage of True Positive (TP), False Negative (FN), False Positive (FP), and True Negative (TP) using proposed method.	52
Table 6 Performance Measurement Result	53
Table 7 Mean Square Error (MSE) of Deformed Model compared with model ground-truth using proposed method.	56

Table of Figure

	Page
Figure 1 Anatomy of Human spine.....	7
Figure 2 Comparision of X-ray image and DEXA Image	8
Figure 3 Grayscale image	9
Figure 4 Binary image	10
Figure 5 Kind of structure element of Morphological Operations (b) Structure element type ‘disk’, (c) Structure element type ‘box’, (e) Structure element type ‘ring’, and (a), (d) are others Structure elements.....	11
Figure 6 Example of applying Gabor filter to original grayscale image(a), output of Gabor filtering with $\theta = 0$ (b) and output of Gabor filter with $\theta = 90$ (c) A set of Gabor filters with different frequencies and orientations may be helpful for extracting useful features from an image. In the discrete domain, two-dimensional Gabor filters are given by,.....	13
Figure 7 Structure Element for Connected-Component Labelling	14
Figure 8 Overall of proposed methodology	27
Figure 9 Pattern of horizontal projection process	29
Figure 10 Drawing triagles from peaks point of graph.....	30
Figure 11 Pattern of interested triangles	31
Figure 12 Finding all possible candidate triangles	32
Figure 13 Summarize of Candidates Selection Method.	32
Figure 14 Segmented ROI of human lumbar spine region	33
Figure 15 (a) Original input image and (b) Result from Top-Hat Filtering.....	34
Figure 16 Example of applying Gabor filter to original grayscale image(a), output of Gabor filtering with $\theta = 0$ (b) and output of Gabor filter with $\theta = 90$ (c).....	34
Figure 17 Gabor filtering Method.....	35
Figure 18 Multi-theta Gabor filtering Method.....	35
Figure 19 Output from multi-theta Gabor Filtering (a) and Noise removed image (b)	36
Figure 20 Ellipse-Shape like of human vertebrae pose	36

Figure 21 The first and second component of each objects (a), Apply an ellipse shape using the first and the second components (b), all ellipse with major axis and minor axis.	37
Figure 22 Selected candidates and vertebrae boundary estimation using curve fitting in binary image (a), Selected candidates and vertebrae boundary estimation using curve fitting in grayscale image (b), final output of vertebrae pose estimation (c).....	38
Figure 23 Original AP view (a) and Manually Vertebrae Pose Identification (b).....	38
Figure 24 AP Side vertebrae pose identification manually (a), Lateral side vertebrae identification (b), normalized position of AP Side, and Normalized of lateral side (d)	39
Figure 25 Registration of AP Side and Lateral Side	40
Figure 26 Imported template as scatter plot (a) (b) and (c), surfae plotted template (d), (e) and (f)	41
Figure 27 List of vertex normal (A , List of alpha value default to 1.0 (B), List of geometric vertices (C) , and Polygonal face element (F).....	42
Figure 28 Construction of Human spine from imported template.....	43
Figure 29 Rotation of each vertebrae	44
Figure 30 Result from rotational of each model	44
Figure 31 Original Input (a), output of binarization (b), and result of small object removing (c).....	46
Figure 32 Result of horizontal projection	46
Figure 33 Result of local peaks finding	47
Figure 34 Result of triangular drawing on each local peaks.....	47
Figure 35 Final result of Region of interest segmentation.....	48
Figure 36 Comparison of evaluation.....	50
Figure 37 Comparison of vertebrae pose segmentation's result	54
Figure 38 Ground-truth model (a) and result of proposed method (b)	55
Figure 39 Volume overlap evaluation of proposed model and ground-truth.....	55
Figure 40 Example of Bone Collapse case in AP view (a) and Lateral view (b)	60

CHAPTER 1

INTRODUCTION AND PROBLEM REVIEW

1.1 Introduction

Recently, three-dimensional model (3D) of human vertebrae plays an important role in many clinical routines. It may support the doctor in variety operations and diagnosis such as surgery operation, lesion detection, and 3D visualization and printing. It also acts as tool for communicating between doctor and patients for patient better understanding. In addition, the 3D model can also be used in tele-medical operation which allow an experts to diagnose patients in wilderness area.

Currently, three-dimensional model of human bone can be created from many devices such as Magnetic Resonance Imaging (MRI) and Computed Tomography (CT). MRI is a medical imaging technique used in radiology to form pictures of the anatomy and the physiological processes of the body in both health and disease. MRI scanners require strong magnetic fields, gradients of electric fields, and radio waves in order to generate an image of the organs of the human body. All strong three sources cause some effects to patients such as headache and debility. In addition, use of MRI is sometime high cost operation. Computed Tomography or CT Scanner is another technology for generating human body image. CT is a combinations of cross-sectional (tomographic) X-ray images taken from different angles. On the other hand, patient will absorb 25 – 360 mSv (milli-Sievert) from the CT operation. Normally in nature, human should be absorbed the radiation about 1.5 mSv per one year. It means that, patient with CT operation absorbs twenty times radiation, comparing with the natural absorption. It increases the risk of cancer or other diseases. Thus, to avoid over dose radiation, a low-radiation X-ray scanner should be proper way for the doctor to deliver to the patient in their diagnosis. The low-radiation X-ray scanner is sometime called Dual-Energy X-ray Absorptiometry Scanner or DXA scanner.

DXA Scanner is normally used in a bone mineral density (BMD) measurement process. Two X-ray beams with different energy levels are

aimed at the patient's bones. Different energy levels of the X-ray beam produce multi-level output images. DXA scanner radiates a very small dose, 1-4 μSv ($1.0 * 10^{-6}$ Sv to $4.0 * 10^{-6}$ Sv). An increasing value of absorbed radiation from the DXA to the patient is very tiny value comparing to the radiation value obtained in daily life. Nevertheless, output image produced from low-radiation scanner provides low quality images which difficult to detect, identify, and diagnose the disease happening in the vertebrae pose.

As mention before, image quality is significantly affected to the work of radiologist to correct and identify the boundary of the bone area. If the volume of X-ray is high value, the output image will be a high contrast, high resolution, and clear boundary image. However, the high volume of X-ray may also cause a serious side effects to the patients. In contrast with low volume of X-ray, it produce low contrast, low resolution and unclear output image. This causes the difficulty of automatic diagnosis operations. In the past decade, a number of methods in enhancing, segmenting, and analyzing low quality output image obtained from the X-ray machine have been proposed and published. In addition, various methods of three dimensional deformation of the human lumbar vertebrae bone have been implemented.

Normally, in the three dimensional deformation process consists of two (2) main steps including image pre-processing and deformation steps. In the image pre-processing step composes of three sub-steps which are image enhancement, segmentation, and registration steps. Generally, low contrast image enhancement and segmentation algorithms can be used to improve the quality of the input image and segment the objects from the given background. But for the registration step, adaptive algorithms for segmenting each vertebrae pose needs to be improved. Because not only the quality of the image is low. But also there are variety of lesion such as bone exostoses and bone collapse happening in each segmenting pose. Normally in the literature, image registration comes from the CT images which provide clearly display and highly contrast information to researchers. In this research, two side images, AP and lateral views with low quality image and different dimensions (or sizes) between AP and lateral views, have been used. In addition, an automatics of registration of each vertebrae bone will be proposed. Then, three dimensional

deformation will be visualized in order to help the doctor in his/her diagnosis and interpret the symptom to the patient.

This research consists of three main phases. In the first phase, lumbar section is extracted from the whole lateral spine. In the second phase, pose estimation for each vertebrae is performed. In the final phase, three-dimensional model of vertebrae is deformed.

1.2 Statements of the Problems

There are significant issues of the low resolution vertebral bone image as follows:

- It may lead to incorrect Lumbar areas extraction from Thoracic areas.
- It may lead to incorrect Lumbar vertebrae pose estimation.
- Only two views of lumbar X-ray image is employed to deform.

Low resolution vertebral bone image that cause from using low radiation on X-ray vertebral bone of the patient to avoid the risk of overdose radiation. This kind of image makes it difficult for the specialist to extract vertebrae bone from the image. This is because of the image has a low quality of element in vertebra bone. Thus, the main objective of this dissertation is to work on low radiation image to extract vertebra bone. In this research, contrast adaptive and extracting methodologies are proposed to find the optimal shape of vertebra bone. The problems that are going to be attempted can be classified as follows:

First, in order to correctly extract bone area from lateral view of low radiation vertebrae bone image from X-ray spine bone scan image, triangular analysis is performed to automatically segment region of interest.

Second, after the lumbar area is extracted, the vertebral poses are identified using Multi-theta Orientation Gabor Filter and Geometric Ellipse-shape analysis combined with Principle Analysis (PCA).

Last, once the lateral vertebrae poses are correctly identified, the identified poses are registered with the ground-truth of AP side vertebrae

poses. Then, three-dimensional model of human lumbar vertebrae is deformed.

1.3 Research Objective

- To extract lumbar vertebral area and vertebral pose from low radiation spine bone images automatically.
- To deform three-dimensional model of lumbar vertebrae.

1.4 Scope of the Study

The dataset is provided by local hospital in Burapha University. It is produced from Dual-Energy X-ray Absorptiometry (DXA) scanner.

- This dataset contains 70 of vertebral bone X-ray images in JPG format.
- Image's resolution is 72 dot per inch.
- Lateral image is with 300-400 pixels of width and 600-700 pixels of height.
- AP image is with 600-700 pixels of width and 500-600 pixels of height.

1.5 Research Advantage

- To obtain knowledge of how to process a wide variety of images and applied research effectively.
- To gain an efficient algorithm for segmenting lumbar region of lateral vertebral body.
- To deform efficiency three-dimensional model of lumbar vertebrae.

CHAPTER 2

THEORETICAL BACKGROUND AND RELATED LITERATURE

2.1 Theoretical Background

2.1.1 Anatomy of the Spine

The spine is made of 33 individual bones stacked one on top of the others. Ligaments and muscles connect the bones together and keep them aligned. The spinal columns provide the main support for your body, allowing you stand upright, bend, and twist. Protected deep inside the bones, the spinal cord connects your body to the brain, allowing movement of your arms and legs. Strong muscles and bones, flexible tendons and ligaments, and sensitive nerves contribute to a healthy spine. Yet, any of these structures affected by strain, injury, or disease can cause pain.

The vertebrae are the 33 individual bones that interlock with each other to form the spinal column. The vertebrae numbered and divided into regions: cervical, thoracic, lumbar, sacrum, and coccyx. Only the top 24 bones are moveable; the vertebrae of the sacrum and coccyx are fused. The vertebrae in each region have unique features that help them perform their main functions such as:

- Cervical (neck) – the main function of the cervical spine is to support the weight of the head (about 10 pounds). The seven cervical vertebrae are number C1 to C7. The neck has the greatest range of motion because of two specialized vertebrae that connect to the skull. The first vertebra (C1) is the ring-shaped atlas that connects directly to the skull. This joint allows for the nodding or “yes” motion of the head. The second vertebra (C2) is the peg-shaped axis, which has a projection called the odontoid, that the atlas pivots around. This joint allows for the side-to-side or “no” motion of the head.

- Thoracic (mid back) the main function of the thoracic spine is to hold the rib cage and protect the heart and lungs. The twelve thoracic vertebrae are numbered T1 to T12. The range of motion in the thoracic spine is limited.
- Lumbar (low back) the main function of the lumbar spine is to bear the weight of body. The five lumbar vertebrae are numbered L1 to L5. These vertebrae are much larger in size to absorb the stress of lifting and carrying heavy objects.
- Sacrum the main function of the sacrum is to connect the spine to the hip bones (iliac). There are five sacral vertebrae, which are fused together. Together with the iliac bones, they form a ring called the pelvic girdle.
- Coccyx – the four fused bones of the coccyx or tailbone provide attachment for ligaments and muscles of the pelvic floor.

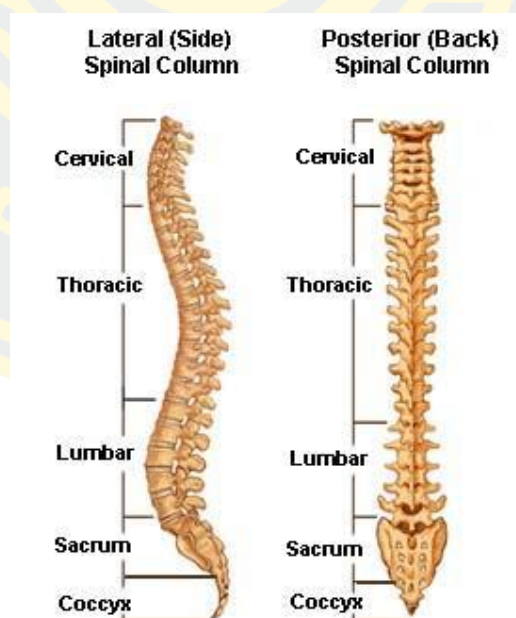


Figure 1 Anatomy of Human spine

2.1.2 Low radiation image

X-ray images from DXA machine are obtained from irradiation through the patient's body. Typically, the dose of radiation on the human body can be determined which will offer different results. If the volume of X-ray is high, the author will get a high-resolution image that the vertebral spine boundary can be seen clearly such as image (a) in Figure 4. The image quality is significantly affected the work of radiologist to correctly identify the boundary of the bone area. However, the high volume of X-ray may also cause a serious effects to the patients such as cancer and tumor. X-ray images of vertebral spine are the main source to predict or diagnose vertebral diseases such as osteoporosis, osteopenia, and scoliosis. To avoid the certain side effects, the radiologist chooses to radiate the low volume of X-ray and obtains the low resolution X-ray images such as image (b) in Figure2

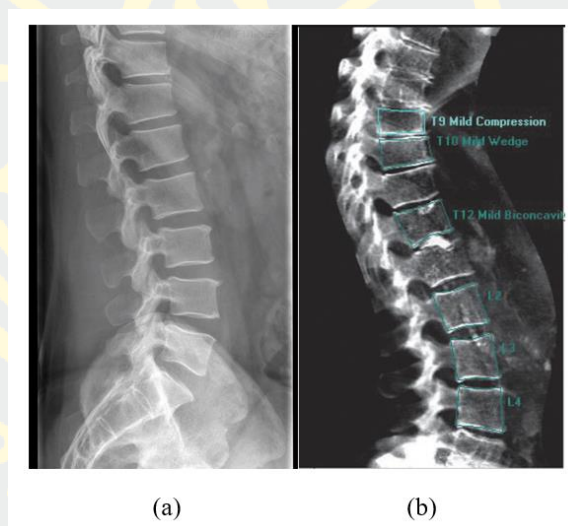


Figure 2 Comparison of X-ray image and DEXA Image

2.1.3 Image Segmentation

Image segmentation is useful in many applications. It can identify the regions of interest in the data. The goal of segmentation is to simplify and/or change the representation of an image into something that is more meaningful and easier to analyze. Image segmentation is typically used to locate objects and boundaries (lines, curves, etc.) in images. More

precisely, image segmentation is the process of assigning a label to every pixel in an image such that pixels with the same label share certain characteristics.

In this research the author categorize the basic existing segmentation as follow this.

- Point, line, and edge Detection
- Thresholding
- Region-Base Segmentation
- Segmentation Using Morphological Operation

In this study, the author is just examples of some basic principles that were used in this research only.

2.1.4 Thresholding

Thresholding is used to segment an image by setting all pixels whose intensity values are above a threshold to a foreground value and all the remaining pixels to a background value. Thresholding is the simplest method of image segmentation. From a grayscale image, thresholding can be used to create binary images by turning all pixels below some threshold to zero and all pixels about that threshold to one is defined as equation (2-4). In Figure 5, 6 and 7 show that the process of thresholding.

$$I(x, y) = \begin{cases} 1, & I(x, y) < T \\ 0, & I(x, y) \geq T \end{cases} \quad (1)$$

where $I(x, y)$ is input image in position x and y . T is threshold value.



Figure 3 Grayscale image

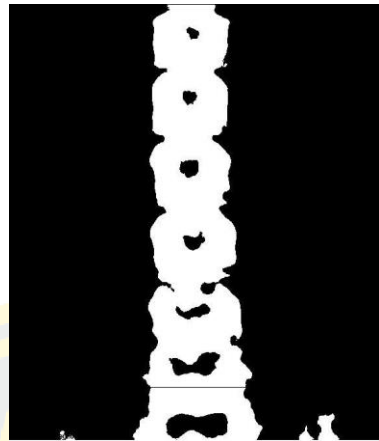


Figure 4 Binary image

2.1.5 Morphological Operation

Binary images may contain numerous flaws. In particular, the binary regions produced by simple thresholding are distorted by noise and texture. Morphological image processing pursues the goals of removing these imperfections by accounting for the form and structure of the image. These techniques can be extended to greyscale images.

Morphological image processing is a collection of non-linear operations related to the shape or morphology of features in an image. Morphological operations rely only on the relative ordering of pixel values, not on their numerical values, and therefore are especially suited to the processing of binary images. Morphological operations can also be applied to greyscale images such that their light transfer functions are unknown and therefore their absolute pixel values are of no or minor interest. The morphological techniques probe an image with a small shape or template called a structuring element. The structuring element is positioned at all possible locations in the image and it is compared with the corresponding neighborhood of pixels as follows Figure 9.

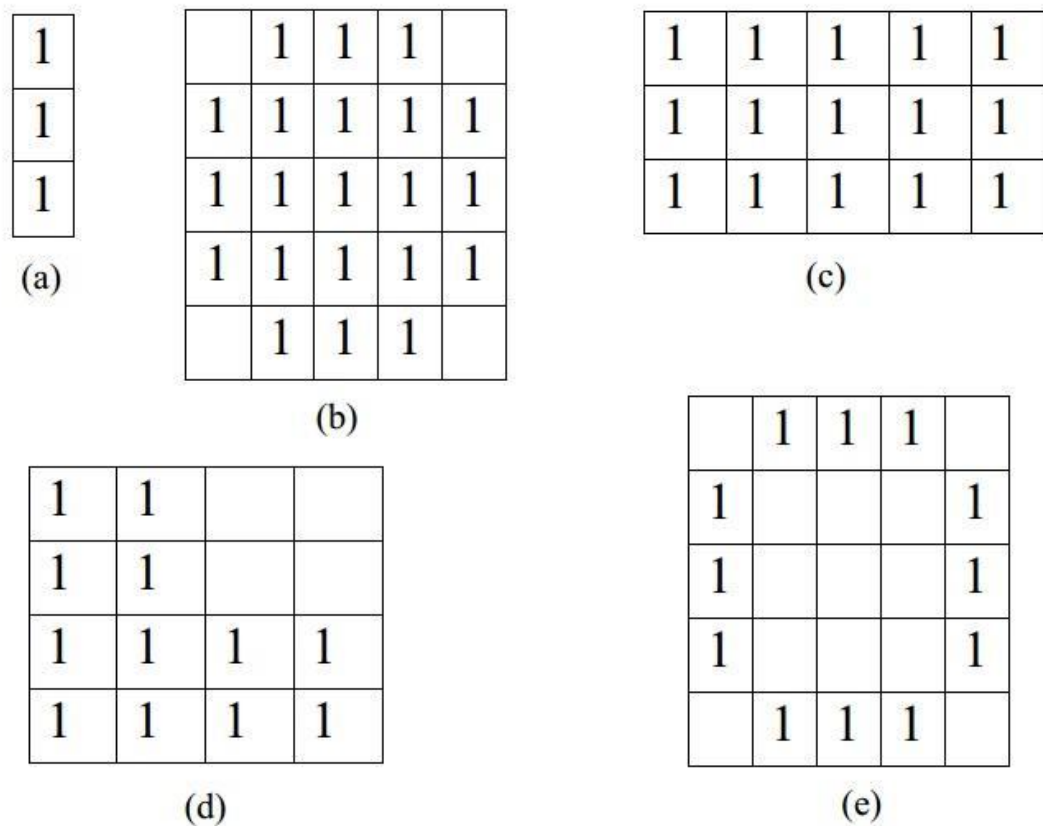


Figure 5 Kind of structure element of Morphological Operations (b) Structure element type 'disk', (c) Structure element type 'box', (e) Structure element type 'ring', and (a), (d) are others Structure elements.

Dilation is one of the basic operations in mathematical morphology. Originally developed for binary images, it has been expanded first to grayscale images, and then to complete lattices. The dilation operation usually uses a structuring element for probing and expanding the shapes contained in the input image is defined as equation (2-5).

$$AB = \bigcup_{b \in B} A_b \quad (2)$$

where A_b is the translation of A and B , and \oplus is dilation operation.

Erosion is one of the two basic operators in the area of mathematical morphology, the other being dilation. It is typically applied to binary images. The basic effect of the operator on a binary image is to erode away the boundaries of regions of foreground pixels. Thus areas of

foreground pixels shrink in size, and holes within those areas become larger is defined as equation (2-6).

$$A \ominus B = \{x | (B)_x \subseteq A\}$$

where A is input image, B is structure element, and \ominus is erosion operation.

Closing is an important operator of the field of mathematical morphology. Like its dual operator opening, it can be derived from the fundamental operations of erosion and dilation. Like those operators it is normally applied to binary images. Closing is similar in some ways to dilation in that it tends to enlarge the boundaries of foreground (bright) regions in an image (and shrink background color holes in such regions), but it is less destructive of the original boundary shape. As with other morphological operators, the exact operation is determined by a structuring element. The effect of the operator is to preserve background regions that have a similar shape to this structuring element, or that can completely contain the structuring element, while eliminating all other regions of background pixels is defined as equation (4)

$$(A \oplus B) \ominus B \quad (4)$$

where A is input image, B is structure element, \oplus is dilation operation, and \ominus is erosion operation.

2.1.7 Gabor Filter

In image processing, a Gabor filter, named after Dennis Gabor, is a linear filter used for texture analysis, which means that it basically analyses whether there are any specific frequency content in the image in specific directions in a localized region around the point or region of analysis. Frequency and orientation representations of Gabor filters are claimed by many contemporary vision scientists to be similar to those of the human visual system, though there is no empirical evidence and no functional rationale to support the idea. They have been found to be particularly appropriate for texture representation and discrimination. In the spatial domain, a 2D Gabor filter is a Gaussian kernel function modulated by a sinusoidal plane wave.

Gabor filters have been used in many applications, such as texture segmentation, target detection, fractal dimension management, document analysis, edge detection, retina identification and image representation. In

the spatial domain, a 2D Gabor filter is a Gaussian kernel function modulated by a sinusoidal plane wave. By using Gaussian and Sine wave, allow us to extract objects in image with specific orientation.

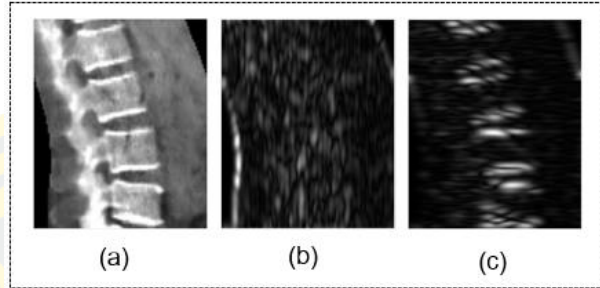


Figure 6 Example of applying Gabor filter to original grayscale image(a), output of Gabor filtering with $\theta = 0$ (b) and output of Gabor filter with $\theta = 90$ (c) A set of Gabor filters with different frequencies and orientations may be helpful for extracting useful features from an image. In the discrete domain, two-dimensional Gabor filters are given by,

$$I_{gb}(\theta) = \sum_u \sum_v (I_{x-u,y-v}) G_{u,v}(\theta) \quad (5)$$

Let I_{gb} is a Gabor filtered image, $I_{x-u,y-v}$ is an original image and $G_{u,v}$ is a Gabor filter with size of $u \times v$. Gabor filter can be described in Eq. 6 below.

$$G_{x,y}(\theta) = e^{\left\{ -\frac{1}{2} \left(\frac{x^2}{\sigma_x^2} + \frac{y^2}{\sigma_y^2} \right) \right\}} \cos(2\pi f x) \quad (6)$$

x and y Can be defined as:

$$\begin{aligned} x &= x \cos \theta + y \sin \theta \\ y &= -x \sin \theta + y \cos \theta \end{aligned} \quad (7)$$

Where f is a modulation of frequencies, σ_x is a Gaussian boundary in x axis and σ_y is a Gaussian boundary in y axis.

2.1.8 Top-Hat Filtering

Top-Hat filter are used to enhance the contrast of images through morphological methods. By subtracting an original image with opening operated image, will show a removed small object with darker image as

defined in Eq. 1. First, start with image erosion for object size reduction, then dilate the image to increase the object size and small object removing.

$$I_{TH} = I - (I \circ S)$$

Let I_{TH} is an image with top-hat filtered, I is an original image, S is a disk-shaped structure element and $I \circ S$ is an opened image by structure element. The opening operation can be described

$$I \circ S = (I \ominus S) \oplus S \quad (9)$$

Let $I \ominus S$ and $I \oplus S$ is an eroded image and dilated image respectively. Image erosion and image dilation can be defined below.

$$I \ominus S = \min_{u,v} \{I_{x+u,y+v} - S_{u,v}\} \quad (10)$$

$$I \oplus S = \max_{u,v} \{I_{x+u,y+v} - S_{u,v}\} \quad (11)$$

Let x, y is a coordinates of an original image and u, v is a coordinates of disk-shaped structure element.

2.1.8 Connected Component Labelling

Connected-Component is an algorithm which apply from graph theory, where subsets of connected components are uniquely labeled based on a given heuristic. Connected-component labeling is used in computer vision to detect connected regions in binary images by using structure element as shown in Fig. 4. In 2-dimensional binary data. The algorithm makes two passes over the image. The first pass to assign temporary labels and record equivalences and the second pass to replace each temporary label by the smallest label of its equivalence class.

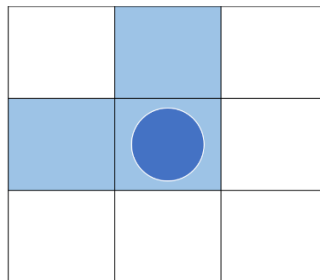


Figure 7 Structure Element for Connected-Component Labelling

2.2 Literature Review

Duarte Barbieri et al (2015, pp. 44-49) studied “Vertebral Body Segmentation of Spine MR Image Using Superpixels {Barbieri, 2015 #1}”. His paper presented a segmentation approach guided by the user for extracting the vertebral bodies of spine from MRI image. The proposed approach, called VBSeg (Vertebral Body Segmentation). The VBSeg aims at segmenting the vertebrae L1, L2, L3, L4 and L5 of the human spinal, receiving as input the Spinal MR Image and five points manually selected by the user, such that each vertebra has one of these points in your area. In this proposed method, there are four main steps. Firstly, they given a Spine MR Image, the specialist selects five points that correspond to the relevant lumbar vertebral bodies to be segmented. Secondly, they take advantage of superpixels to cluster homogeneous pixels to reduce the image complexity and then making easy the detection of each vertebral body contour. Superpixels adapt themselves to the structure of images. However, for some diseases or abnormalities, the boundary of each superpixel does not fit well in the vertebra contour. Thirdly, to avoid missing important boundaries of the vertebral bodies, they propose to use the Otsu’s method as a pos-segmentation step to divide the superpixels into smaller ones. Finally, the final segmentation they use a region growing approach using points manually selected by the specialist. In the first step of this paper, the aid of the specialist must be necessary, because it avoids detecting false vertebrae considered not relevant in the diagnostic of the pathology. In the following his detail the other steps of the proposed approach. From the experiment result they can produce masks of the five lumbar vertebrae with an average precision of 80%, jaccard index of 71% and recall of 87%, when compared to the manual segmentation of a trained specialist. These values show that the VBSeg is a valuable asset to assist the medical specialist in the task of vertebral bodies very much. In this paper has a strong and weak in this paper which you can following this. The strong in this paper, it can extracting normal bone case with 100%. The weakness in this paper, their proposed approach is semi-automatics and it can extracting worst bone case with 66%.

R. Peter et al (2013, pp. 2376-2379) studied “3D CT spine data segmentation and analysis of vertebrae bone lesions”. In this paper, they proposed a methodology for detecting and classifying bone lesions in 3D CT data of human spine images. This problem consists basically of two components. Firstly, to segment spine they use 3D intensity models of the individual types of vertebrae that has been prepared by averaging healthy vertebra image data. Using these models, accordingly modified for each individual vertebra, the concrete patient’s spine is segmented into separated vertebrae, subsequently then submitted to the analysis of lesions from minimum intersection of corresponding vertebrae to maximum intersection. From the model of vertebrae they use 22 models of individual types of vertebrae (six cervical, twelve thoracic and four lumbar) derived ahead, are the key concept in the presented segmentation approach. On the difference to previous work where the shape models are formulated as triangulated meshes, their models are 3D intensity data, derived by averaging of a number of normalized and registered healthy cases of the concrete vertebra type. Then, lack of distinct texture inside lesions in the CT spine data makes the process of metastases classification difficult; none of the run-length coding, co-occurrence matrices, local binary patterns or Fourier-based methods have provided relevant features. Therefore, only local mean intensities could have been so far considered. To verified differences of local mean intensity within the metastatic tissues with respect to the surrounding healthy tissue enabled to use the classification model based on Bayesian distribution combined with Markov random field (MRF) technique. From experiment result, in the segmentation phase, 320 vertebral bodies were segmented with rate of accurate results in 82 % with moderately deformed vertebrae and in 53% in heavily distorted ones. Similarly, small local inaccuracies have been found in about 10% (28% in the last group). It seems to surpass the so far reported results. With respect to the method of lesion analysis, it is positive that the presented algorithm is able to classify metastases of various sizes; from 5 voxels up to many hundreds of voxels. The sensitivity and specificity of the lesion analysis was evaluated separately for hypo-dense metastases with sensitivity 55.7% and specificity 91.4%; similarly for hyper-dense metastases they were 63.5% and 95.1%, respectively.

Ruiz-Espana et al (2015, pp. 3049-3052) studied “A Fully Automated Level-Set Based Segmentation Method of Thoracic and Lumbar Vertebral Bodies in Computed Tomography Images”. His paper presented a fully automatic segmentation method of thoracic and lumbar vertebral bodies from 3D Computed Tomography (CT) image. Then, from 3D input image they convert 3D to 2D image using cross-section technique for used to analyze region of interest (ROI). Because, identification and segmentation of the vertebral structures are of relevance to many medical applications related to the spine, such as diagnosis, therapy or surgical intervention. However, the development of automatic and reliable methods are an unmet need. The procedure of this paper can be divided into four main stages. Firstly, the spinal detection to find the seed point automatically which in this step have three sub main steps. First step is to set a high contrast between the spinal canal and cortical bone and perform a set of morphological operations to find voxels belonging to the spinal canal. Second step is to extract only those 3D objects constituting spinal canal and, finally, a centroid extraction for each slice of spinal canal object is performed. Besides, interpolation and extrapolation of data is carried out as, due to the morphological operations executed in first step, not all the slices are present in the spinal canal object to generate initial contours in the segmentation process, automating the whole process. Secondly, they use the centroid from previous step to create a circular region of interest (5.5 cm radius) for remove unwanted object in the image and improve the image quality and make the segmentation results more accurate by gamma correction technique. Thirdly, they use the Selective Binary Gaussian Filtering Regularized Level Set method to identify the contour of the thoracic and lumbar vertebral bodies effectively. Finally, two morphological operations were applied in order to refine the segmentation result for getting more correctly. The method was tested in clinical data coming from 10 trauma patients. To evaluate the result the average value of the DICE coefficient was calculated, obtaining a 90.86 ± 1.87 % in the whole spine (thoracic and lumbar regions), a 86.08 ± 1.73 % in the thoracic region and a $95,61 \pm 2,25$ % in the lumbar region. The results are highly competitive when compared to the results obtained in previous methods, especially for the lumbar region.

Zhentai Lu et al (2012, pp. 1240-1243) studied “Adaptive image segmentation Based on local neighborhood information and Gaussian weighted chi-square distance”. In this paper they proposed a novel affinity matrix for brain and spine image segmentation. The affinity matrix is created by Gaussian weighted chi-square distance from neighborhood data, such the region of interest of the brain and vertebral bodies in the image. In this paper they proposed the graph-based segmentation approach to solve the automatic segmentation of the vertebral bodies from sagittal magnetic resonance images of the spine is directly impacted by the affinity matrix and compare his method between NJW and the gamio algorithm. NJW algorithm is a methodology to segment the objects with the use of the intensity of each pixel but without considering the neighborhood pixels. The intensities of the vertebral bodies are similar to those of the fat around the vertebral bodies so this method is most likely to lead to the phenomena of over-segmentation in the joint location. Then the gamio algorithm, this algorithm uses the window histograms of intensity as the most promising features, thereby missing the spatial information. Moreover, it uses a single scaling parameter so that the segmented results are poor. This algorithm performed well in the vertebral bodies showing high contrast with respect to the intervertebral discs and surrounding structures in the T1-weighted images. However, the performance was poor if the condition was not satisfied. The algorithm’s performance degraded when they tested far from the mid-sagittal slice. Moreover, this algorithm cannot obtain good segmented results in T2 high-resolution images. Finally, they propose the self-acting segmentation method for vertebral bodies and brain image. It has encouraging results on the location of the intensities of the vertebral bodies, which are similar to the tissues around the vertebral bodies. The phenomena of over-segmentation and under-segmentation can then be restrained. This improved algorithm segments the vertebral bodies smoothly, clearly, and accurately. From experiment result, their approach obtain the robustness result when compared with NJW and the gamio algorithm.

Ruiz-Espana, Domingo et al (2015, pp. 2014-2017) studied “Automatic Segmentation of the Spine by Means of a Probabilistic Atlas with a Special Focus on Ribs Suppression. Preliminary Results”. In this paper they proposed the methodology for segmenting vertebral body

image automatically. However, automatic and detailed segmentation of vertebrae is a challenging task, especially due to the proximity of the vertebrae to the corresponding ribs and other structures such as blood vessels. So, to overcome these problems, a probabilistic atlas of the spine, including cervical, thoracic and lumbar vertebrae has been built to introduce anatomical knowledge in the segmentation process, aiming to deal with overlapping gray levels and the proximity to other structures. In this research they have many steps. Firstly, from a set of 3D images 10 data sets have been selected and manually segmented to be used as ground truth (6 for training and 4 for testing) and convert these data set to 2D image with cross-section technique. Then, they find the central points at each slice constitutes a curve by the 'guiding curve' technique from previous work. Then, they remove unwanted objects from each slide by thresholding technique and they generate the altars probability in order to increase accuracy for remove unwanted object effectiveness. Finally, to perform an initial segmentation of the spine a fully automated method for vertebrae segmentation from seed points detected automatically in the spinal canal was used Gaussian Filtering Regularized Level Set method to get the most accurate result. From experiment result they computed the Hausdorff distance between the manually-segmented ground truth and an automatic segmentation and also between the ground truth and the automatic segmentation refined with the atlas. The results are promising, obtaining a higher improvement especially in the thoracic region, where the ribs can be found and appropriately eliminated.

Aslan, Shababy et al (2013, pp. 840-843) studied "Clinically desired segmentation method for vertebral bodies". In this paper, they proposed a clinically desired a semi-automatic segmentation method for vertebral bodies (VBs) in computed tomography (CT) images for diagnosis any disease in task of medical image with uses limited interventions only in the VB separation process. They found that, three pieces of information (intensity, spatial interaction, and shape) are modeled to optimize a new probabilistic energy functional; and hence to obtain the optimum segmentation. The information of the intensity and spatial interaction are modeled using the Gaussian and Gibbs distribution, respectively. A shape model is proposed using a new probabilistic function to enhance the segmentation results. Then, they generate a model from this information which is obtained using the cervical, lumbar, and

thoracic spinal regions. Then, from spatial interaction information that describes the relation between pixels is modeled using a Markov Gibbs random field (MGRF). From the experiment result, they use many coefficient to measurement accuracy of this paper such as Accuracy, Precision, Jaccard, and Dice coefficient. The overall segmentation process completes the task in very low execution time which is one of the most important contribution of this paper. Moreover, this research reveals that the proposed method is robust under various noise levels, less variant to the initialization, and quite faster than alternative methods and can be suitable for the clinical works with acceptable results.

Ruiqiong Shi, Dongmei Sun et al (2007, pp. 713-717) studied “An Efficient Method for Segmentation of MRI Spine Images”. In this paper they proposed the automated MR vertebral disks image segmentation system. Their method can locate and label the disks through locating the spinal cord consist of four main steps. Firstly, they select the clearest image in vertebra disks and spinal cord of the sequence because low contrast along with the background noise in MR images make it difficult for distinguishing between the spine tissues and its background. So preprocessing of original image should be implemented before extracting spinal cord. Secondly, for preprocessing step they enhance the contrast of the image firstly, and then apply a 3-by-3 median spatial filter because of its demonstrated ability to reduce random noise without blurring edges as much as a comparable linear low-pass filters. Thirdly, In order to extract spinal cord from a complex scene, we use statistical pattern recognition method to shrink the region of the spinal cord for further processing. Images sequences from 10 patients are chosen as the training set in this step. Then, they use Hough Transform technique to locate and label the disks through locating the spinal cord effectively. Finally, in disk detection section they describe our method to performing disks detection. To tracking disks they use a self-adaptive rectangle window, which is tangent to the contour of the disk, to locate the area of the disk. The tracking action is started by hand-labeling the position of the first disk, the following disks will be tracked along the trend of the spine coil one by one with the same procedure automatically. Then, the efficiency of the proposed method is demonstrated by experiments using real MR images provided by College of Medicine, University of Cincinnati.

Melih S. Aslan, Aly A. Farag et al (2011, pp. 2010-2013) studied “Segmentation of Vertebrae using Level Sets with Expectation Maximization algorithm”. In this paper, they proposed a robust level sets method to segment vertebral bodies (VBs) in clinical computed tomography (CT) images. Since the VB and surrounding organs have very close gray level information and there are no strong edges in some CT images. So, the initialization of level sets method becomes very crucial step. Sometimes the object and background regions are not initialized correctly, the results would not be acceptable. Also, the size and place of the initial seed may give non-reproducible results. So, to solve these problems in this research, they use a statistical level sets method which uses the Expectation Maximization (EM) algorithm for the initialization and parameter estimation. From initializing the seed point of level set method starts by initializing the level set function as the signed distance function of a circle centered at seed point(s) that can be either manually placed by the user or automatically selected. From parameter estimation they use the region information and means of gradient descent follow by Bayes’ rule to estimate parameter of this paper. For experiment result Validity was analyzed using ground truths of data sets (expert segmentation) and the European Spine Phantom (ESP) as a known reference. The proposed method is compared with other known alternatives such as Min error%, Max error%, Mean error%, and Standard derivation error%. For example the average error of the VB segmentation on 10 clinical image sets is 3.2% for the proposed method. Moreover, the segmentation time is much faster than other previous method.

Luc Duong, Farida Cheriet et al (2010, pp. 1143-1151) studied “Automatic Detection of Scoliotic Curves in Posteroanterior Radiographs”. In this paper they proposed a new method for automatic detection of spinal curves from a Poster Anterior (PA) radiograph. In this study they have many steps. First, initial identification of one region of interest (ROI) per vertebral level is introduced, based on a set of radiographs with manually. From this manual identification, ROI for each vertebral level are identified using the relative 2-D locations of spine landmarks cumulated from 100 PA radiographs. Insert shows the ROI of T8 vertebral level. Then, from ROI they identify the characteristic curve (S or C shape) of vertebrae with Cobb angle technique. From identification ROI step in pre-processing process they use the shock filter

to enhance those anatomical structures while reducing radiographic noise in the surrounding area. Second, features extraction and classification step they use a statistical classifier based on SVMs with a Gaussian kernel is introduced to build a knowledge-based detection scheme able to discriminate the spine region from the rest of the radiograph. SVMs are renowned for their usefulness in solving two-class problems, and thus highly suitable for our application, which consists in distinguishing regions within the spine from those outside the spine in radiographic images. Finally, the result of this paper was validated by cluster analysis, using expectation maximization (EM) algorithm. Cluster analysis showed that difference between cluster centers was not significantly discriminative in the linear space. Classification rate, using the cluster center as reference, ranged from 50% to 60% of positive classification. However, results from EM clustering showed that the standard deviation associated with the cluster center was overall reduced, suggesting a denser distribution, in the linear space.

Sabine Bauer and Urs Buchholz (2013, pp. 158-163) studied “Biomechanical Effects of Spinal Fusion to Adjacent Vertebral Segments”. In this paper they proposed a 3D Multi Body Simulation (MBS) model of the lumbar spine with realistic surfaces of vertebrae and correct positioning relative to each other which is based on computer tomography (CT) measurement and segmentation processes. To generate MBS model they have many steps in this paper. Firstly, in the generation of vertebrae surface process they use the templates of the body surfaces from artificial vertebrae, which represent the average size of the image for mesh smoothing and reduce the amount of data. So that after the implementation of the surfaces of the MBS model a fast calculation time is guaranteed. The positioning of the vertebral bodies can follow the criterion that endplates of the corresponding vertebral bodies superimpose in the lateral direction and in sagittal. Secondly, in the modeling of intervertebral disc they consider the behavior of force in the intervertebral take from previous work. Then, they identify the characteristic curve for each direction. They are calculated following the results of experimental measurements of isolated postmortem disc material from previous study in order to simulate the contact between the corresponding articular surfaces. Finally, with this model the loads on the different structure, before and after spinal fusion of the functional unit L5-L4, are calculated

to show the biomechanical effects to adjacent vertebral segments under different loaded case. From experiment result, the comparison of the simulations shows a redistribution of loads within the spinal structures. In the simulation case of spinal fusion, the posterior structures are more loaded than in the simulated healthy state. The validation of the model was carried out by comparing the result with FE simulations, various in vitro experiments and experimental data from biomedical literature.

Huang and Chao-Hui (2013, pp.1-5) studied “Pose Estimation for Vertebral Mobility Analysis using eXclusive-ICA based Boosting (XICABoost) Algorithm”. In this paper they proposed an automated vertebral pose estimation based on the given two sets of training patterns. The first set contains the images of vertebrae, in which all vertebral columns are fixed in a proper pose; the second is the images which are cropped with arbitrarily shift and rotate. Based on these two pattern sets, the proposed method can perform template matching. By using exhaustive searching, they will be able to estimate the poses of the vertebral columns on the given X-ray images. The proposed method consists of two parts: First, feature extraction and Second, classification. The first part they extract the unique features from the two given training pattern sets using eXclusive Independent Component Analysis (XICA). Given two sets of training patterns, XICA can obtain the relevant information of differences and resemblance between the given pattern sets. These unique features are used to support the second part, which is a classifier inspired by the famous AdaBoost. It uses the information obtained from XICA. Within a series of iteration, a set of weak classifiers is collected and serve as a strong classifier. In the experiment, they have run robustness tests. The results suggested that with a proper training pattern, the propose XICABoost algorithm can be very sensitive on image shifting and rotation. As a result, it can provide useful information for supporting diagnosis of the relevant medical conditions.

Rabia Hag, David A. Besachio et al (2014, pp. 3191-3196) studied “Using Shape-Aware Models for Lumbar Spine Intervertebral Disc Segmentation”. In this paper they proposed a minimally supervised method for 3D segmentation of herniated discs from high-resolution T2-weighted Magnetic Resonance Imaging (MRI). From methodology they start with pre-processing. In preprocessing the anisotropic filter has been applied to the volumetric images to reduce image noise within the

structures while preserving image boundaries. The filter mitigates image noise located around the disc by reducing the overlapping image intensities of the herniated disc boundary and the surrounding posterior ligament. The Insight Segmentation and Registration Toolkit (ITK) has been utilized for applying image preprocessing filters. Then, in the mesh initialization through landmark-based affine registration step. An ellipsoid template mesh is initialized within the herniated disc image volume for simplex mesh deformation. Arbitrary translation, rotation and scaling effects need to be captured between the template mesh and the MRI image. 6 landmarks are manually placed on the ellipsoid template mesh corresponding to 6 landmarks within the disc image boundary to initialize the template within the disc image through affine registration. These landmarks are placed at the center, superior, inferior, anterior and posterior points on the disc surface, as well as at the mostly superior disc surface to capture arbitrary rotational effects. Then, they use the constant connectivity of the 2-simplex mesh leads to three simplex parameters corresponding to a vertex with a mass and its three neighboring vertices that are invariant under similarity transformations for automatic multi-resolution simplex deformation. Then, User-guided pathology segmentation is manually guided by placing internal and external constraint points on the volumetric image that gracefully constrain the deformation to correct under and over segmentation. Constraint point forces are enforced as an addition to the external force. Finally, from experiment result they use Average results of 5 herniated discs comparing minimally supervised segmentation results against manual segmentation have been calculated. Evaluation results have been obtained by calculating surface to mesh difference between the manual segmentation, considered ground truth, and simplex model from our approach of the corresponding intervertebral disc. Our approach demonstrates absolute mean surface error of $0.61 \text{ mm} \pm 0.52 \text{ mm}$.

Raja' S. Alomari, Jason J. Corso et al (2011, pp. 1-10) studied "Labeling of Lumbar Discs Using Both Pixel- and Object-Level Features with a Two-Level Probabilistic Model". In this paper they proposed a two-level probabilistic model for the localization of discs from clinical magnetic resonance imaging (MRI) data that captures both pixel- and object-level features. They start from analyzed the relation between proton density and age in normal discs. Next, they discuss the related

work stratified by the driving anatomical structure by trend technique from many previous related works: vertebrae, soft tissues, and discs. Then, they developed a two level generative probabilistic such as Conventional Labeling Model and Two-Level Model. In their model, they incorporate two levels of information: low- and high-level. At the low-level, they model the local pixel properties of discs, such as appearance. On the high-level, they capture the object-level geometry and contextual relationships between discs. Our two-level model allows the assumption of conditional independence at the pixel-level to enhance efficiency while maintaining robustness. In experiment result, they have two methods to the measurement result of this research. Firstly, they report a quantitative measure for accuracy of testing on the training set itself and on the rest of the cases (the remaining 55 cases). Then, they consider that the disc is correctly localized if the resulting points lie inside the disc by visually inspecting all the resulting images. We report both training and testing results to show that our model did not over fit on the training data. The accuracy is comparable between the training and the testing set which is around 90%. Secondly, they use 80 abnormal cases: 30 cases for training and the remaining 50 for testing. We perform localization for the testing set only which shows an accuracy over 87% from the summary of statistics of Euclidean distances. Similar to the box plot of the first experiment, whiskers extend from each end of the box to the most extreme values within 1.5 times the inter-quartile range from the ends of the box. Thus, all Euclidean distances larger than 1.5 times the inter-quartile range are considered statistical outliers. By examining both box plots, they notice strong consistency in our labeling results.

R. Sa et. al. proposed a lateral lumbar vertebrae segmentation in scale-variant high radiant X-ray clinical image. E. Alvarez Ribeiro et. al. presented a procedure to detect lumbar vertebral in lateral high-dose of X-ray images using Gabor filter. R. Sa et al. demonstrated a method which use R-CNN to detect intervertebral disc in X-Ray image G. Zheng et al. introduced a method to reconstruct a lumbar vertebral from a single fluoroscopic image.

S. Ghosh et al. proposed a new approach to automate disc localization in clinical lumbar from MRI image using machine learning with heuristics. This research used Histogram of Oriented Gradients (HOG) together with Support Vector Machine (SVM) as classifier. The experimental results

achieved an accuracy rate of 99% for disc localization on 53 clinical cases (318 lumbar discs). Y. J. Zhao et al. presented a method to segment a vertebrae pose using shape of vertebrae spine segment extracted using improved GVF snake. This research proposed a semi-automatic segmentation method in which 12-points (12-anatomical point representation) was manually annotated on the region of interest (ROI) before the ROI on target object can be extracted automatically.

J. Patrick and M. G. Indu proposed a semi-automated method to segment vertebrae on CT images. The vertebral body is identified using iterative Normalized-cut algorithm for detection process which applied eigenvalue decomposition. For segmentation technique, region based active contour method was proposed to segment individual vertebrae. Y. Li et al. proposed an automatic initialized level set approach based on region correlation for lumbar vertebrae segmentation on CT image

CHAPTER 3

METHODOLOGY

In this research, the methodology for three-dimensional model of human lumbar vertebrae deformation is proposed. The proposed method consists of three main phases. In the first Phase, region of interest of human lumbar vertebrae is extracted. In the second phase, lumbar vertebrae poses are estimated. In the last phase, three-dimensional model of lumbar vertebrae is performed. The briefed methodology is demonstrated below:

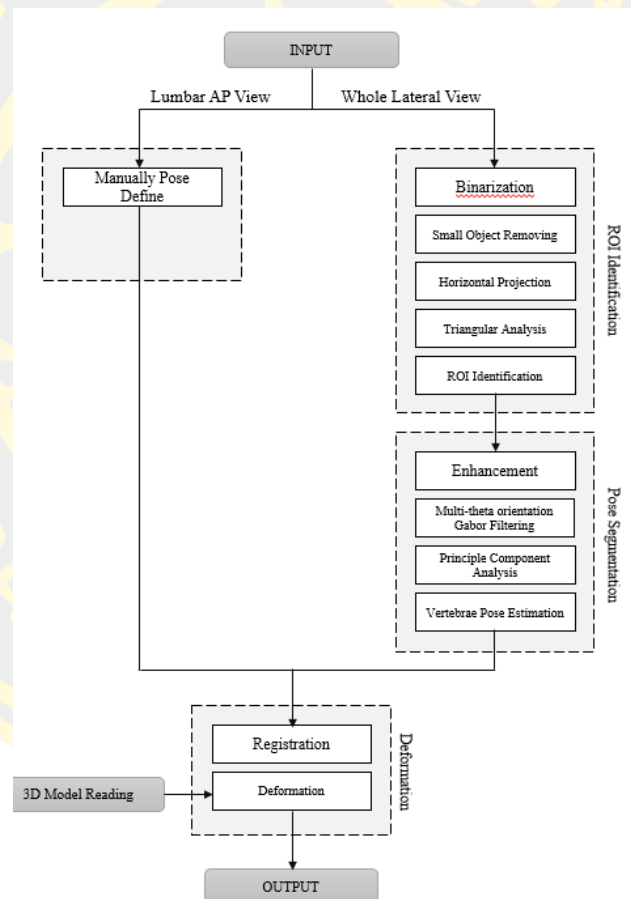


Figure 8 Overall of proposed methodology

3.1 Region of Interest Identification

This phase consists of 3 main steps. Firstly, the input image is converted from grayscale image to binary image using image Information Entropy as threshold value. Then, small objects are removed. Secondly, horizontal projection is performed to reveal a pattern of spine. Then, candidates of lower and upper boundary of lumbar area is chosen using Triangular Analysis. Finally, region of interest of lumbar area is identified.

3.1.1 Binarization

In this study, lateral view radiography image produced from DXA scanner is used as an input image. The binarization process is applied to increase the differentiation between the object of interest and background. In order to make a clear distinction, a technique called “entropy value” proposed by Du-Yih Tsai et. al. is used to measure entropy values of each input image. This value is then set as an initial threshold value to extract foreground from its background. The entropy value is defined by equation

$$E(x) = - \sum_{i=1}^n \sum_{j=1}^m P(x_{ij}) \log_2 P(x_{ij}) \quad (12)$$

Where x is an input image, n is image's width, m is image's height, x_{ij} is intensity in grayscale image and $P(x_{ij})$ is a probability of each x_{ij}

3.1.2 Small objects removing

After the binarization process to extract object of interest from background using entropy information, there still be a number of small unconnected objects remained the image. To remove these small objects, the Morphological Opening Operation is employed as defined in equation

$$A \circ B = (A \ominus B) \oplus B \quad (13)$$

Where A is an input image, B is a specific structure element, \ominus is an erosion operation and \oplus is a dilation operation respectively.

Opening Operation is used to remove small objects from the foreground of an image. In this operation, there are two techniques: Erosion and Dilation. Firstly the Erosion technique is used to remove small object in the foreground which may also remove parts of object of

interes. Thus, after the Erosion step, the Dilation technique is used to restores the eroded part of object of interest. After applying the opening operation, inconsiderable objects are removed.

3.1.2 Horizontal Projection

The output of the pre-processing process as described above, is then projected as a time series graph using horizontal projection. The horizontal projection is a summation of an image's intensity that transform two dimensional information into one dimensional information to reveal pattern of region of interest. The horizontal projection is employed as defined in equation

$$H_k(x) = \sum_{i=1}^n x_{k,i} \quad (14)$$

Where k is an each image's row number, x is an pre-processed input image and n is an image's column number.

The result of horizontal projection can reveal the characteristics of individual parts of the human spine which can later use to determine lumbar section as shown in Figure9 That is, the lumbar section can be clearly spotted by an area where the graph obtained lower peaks as compared with the surrounded peaks or look similar like a valley

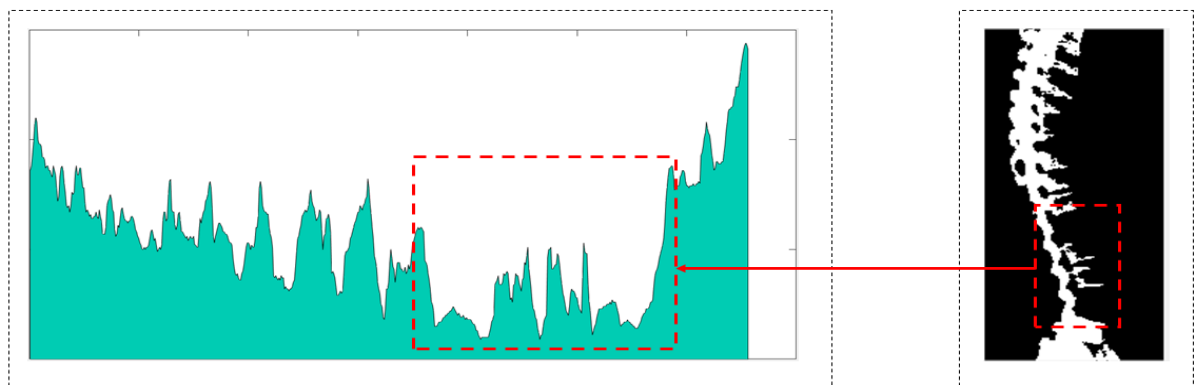


Figure 9 Pattern of horizontal projection process

In order to identify those peaks, the local maxima information is used to locate each peak. The local maxima is calculated as defined in However, an initial result of local maxima calculation provided too many

maxima points or peaks. Therefore, a graph smoothing technique is applied to eliminate those insignificant peaks.

3.1.2 Triangular Analysis

After the local maxima points are identified, the association among peaks are retrieved using triangular shape as shown in *Fig. 4*. Triangular shape is created using a peak with its left and right adjacent peaks. These triangular shape objects are used to locate the valley area.

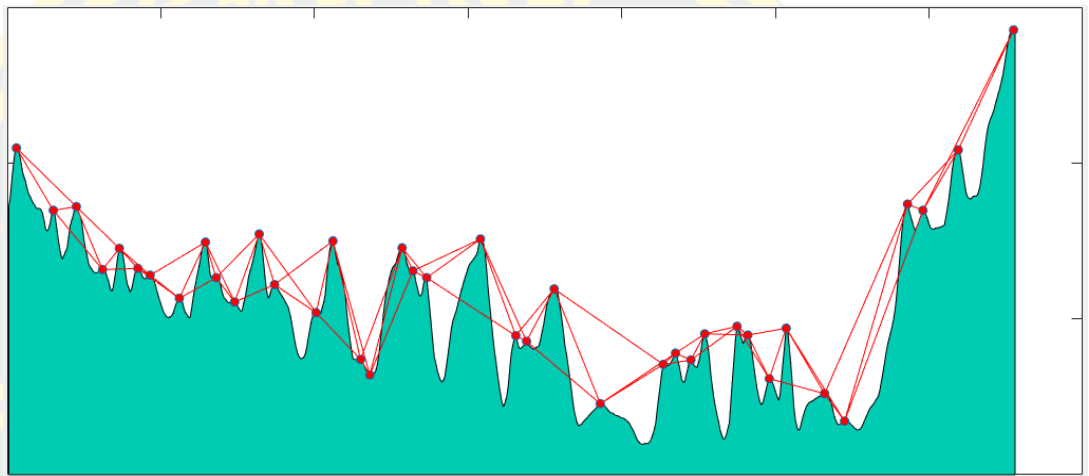


Figure 10 Drawing triagles from peaks point of graph

All triangles that generated from peak points in the former step can be classified into 4 patterns: a) left side peak of an examined point is in quadrant two and right side peak is in quadrant one, b) left side peak of an examined point is in quadrant two and right side peak is in quadrant four, c) left side peak of an examined point is in quadrant three and right side peak is in quadrant one and d) left side peak of an examined point is in quadrant three and right side peak is in quadrant four. From those four patterns of triangles, it clearly demonstrated that pattern d) and c) are patterns that corresponding well to the candidate objects. Thus, these patterns are used to determine lumbar section as shown in Figure11

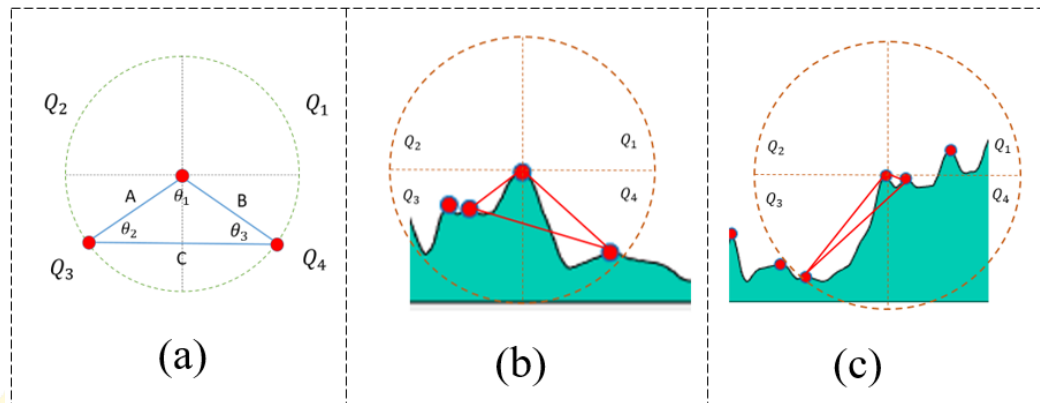


Figure 11 Pattern of interested triangles

However, using located quadrant of each triangle is not enough to identify candidate objects. Thus, another feature is needed to help identify them. The proposed method applied interior angle and triangular length to determine candidates. The interior angles are measured using law of cosine.

From observation, the boundary of lower lumbar section can be determined by θ_2 . In which, the θ_2 has to be an acute angle, where the value of θ_2 has to be in the range of $0 < \theta_2 < 10$. Furthermore, θ_1 has to be an obtuse angle, where the value of θ_1 has to be in the range of $90 < \theta_1 < 180$ as shown in Fig. 5 (c). Then, triangular length of each object is measured and then compared among all candidate objects to locate the one with maximum value or Length A as shown in **Error! Reference source not found.** (b). The selected triangle is then used to locate the lower bound of the lumbar section. Likewise, the determination of candidate object for upper lumbar section is identified by θ_3 where θ_3 has to be an acute angle and its value fall into the range of $0 < \theta_3 < 45$. Furthermore, the θ_1 has to be an obtuse angle where θ_1 fall into the range of $90 < \theta_1 < 180$ as shown in Fig. 5 (b). The candidate objects that got the maximum length B is chosen as a selected triangle that used to locate the upper bound of the lumbar section as shown in Fig.6 (d). Algorithm for finding the candidate objects is illustrated in Figure12

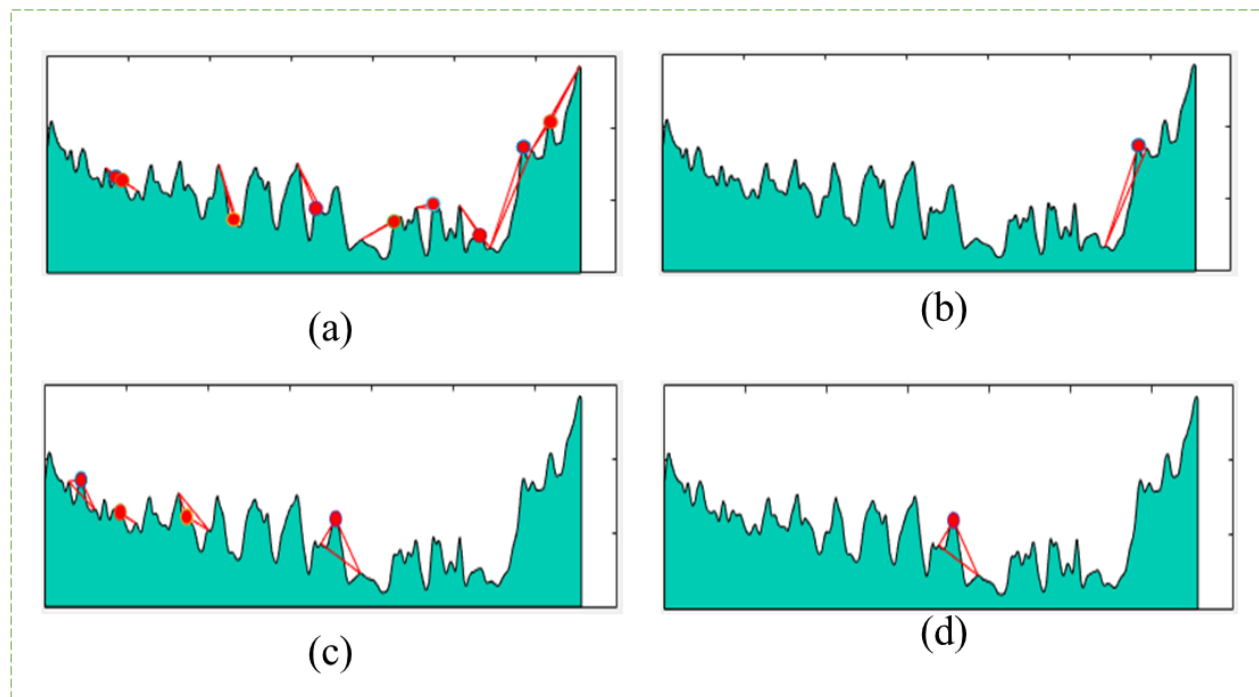


Figure 12 Finding all possible candidate triangles

Algorithm 1 Candidates Selection

Input: Triangles

Output: Boundary

begin

```

1: for  $i = 1 : \text{size}(\text{triangles})$  do
2:    $\text{angles} = \text{anglecalculator}(\text{triangle}(i))$ 
3:    $\text{minangle} = \text{min}(\text{angles}(1))$ 
4:    $n = 1$ 
5:   if  $\text{minangles} \geq 0$  AND  $\text{minangles} \leq 45$  then
6:      $\text{candidates}(n) = \text{triangles}(i)$ 
7:      $n++$ 
8:    $\text{maxdistance} = \text{min}(\text{candidates}(i,2))$ 
9:   for  $i = 1 : \text{size}(\text{candidates})$  do
10:    if  $\text{maxdistance} = \text{candidates}(i,2)$  then
11:       $\text{boundary} = \text{candidates}(i)$ 
end

```

Figure 13 Summarize of Candidates Selection Method.

After obtaining information for locating both upper and lower boundary, these information is then used to segment the lumbar region from original input image as shown in Figure14

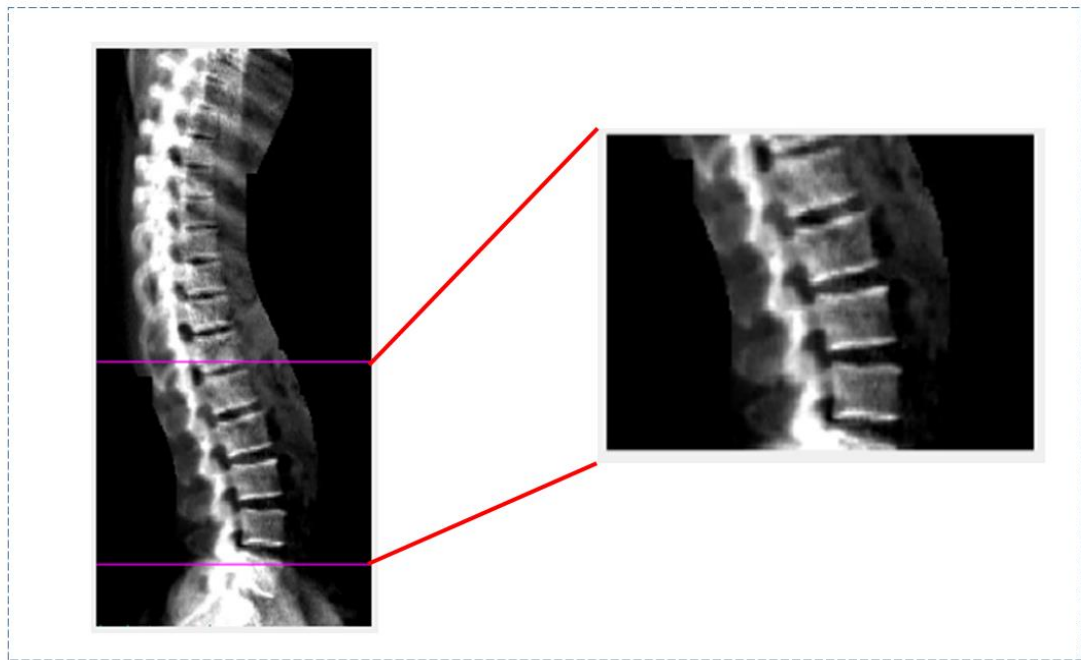


Figure 14 Segmented ROI of human lumbar spine region

3.2 Vertebrae Pose Estimation

In this section, the proposed method to estimate vertebrae pose in low radiation image is briefly demonstrated in Fig.6. The approach start from enhancing an input image using Top-Hat filtering. Then, Multi-theta orientation Gabor filter is employed to extract objects in each specific orientations. After that, insignificantly small objects are removed. Secondly, Geometric Ellipse-shape is created using Principle Component Analysis to determine the vertebrae poses area and each orientations. Finally, the vertebrae poses are identified.

3.2.1 Image Enhancement using Top-Hat filter

According to Eq 8. Since the opening operator leaves a background of the image, it is expected that Top-Hat filter removes the image background. This filter acts like a high-pass filter and extracts the bright areas then remove dark areas of the image as shown in an output image result in Figure15

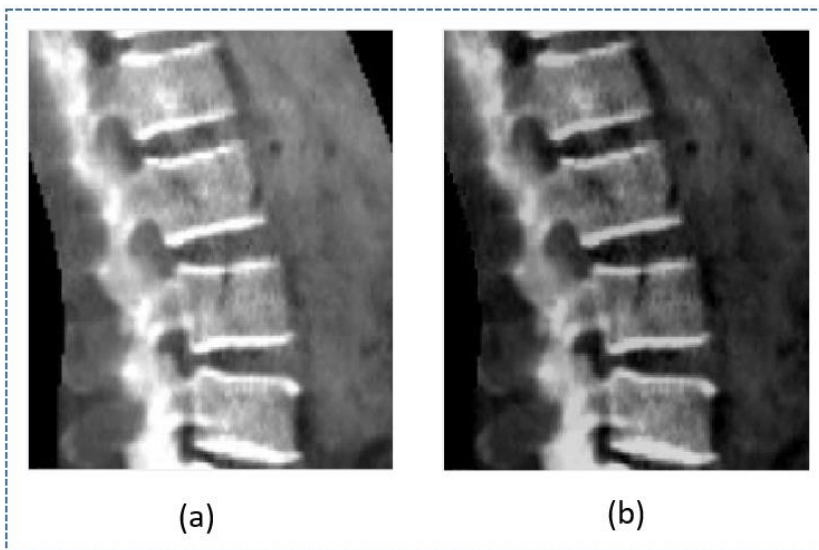


Figure 15 (a) Original input image and (b) Result from Top-Hat Filtering

3.2.2 Multi-theta Orientation Gabor Filter

As shown in Eq. 5 and Eq. 6 Gabor filter is used to extract an object in specific orientation degree. Nevertheless, the interested object (Vertebrae posed) in this dataset appears in variety of orientation degree. Thus, Multi-theta Orientation Gabor filter is employed to extracted object in variety of degrees.

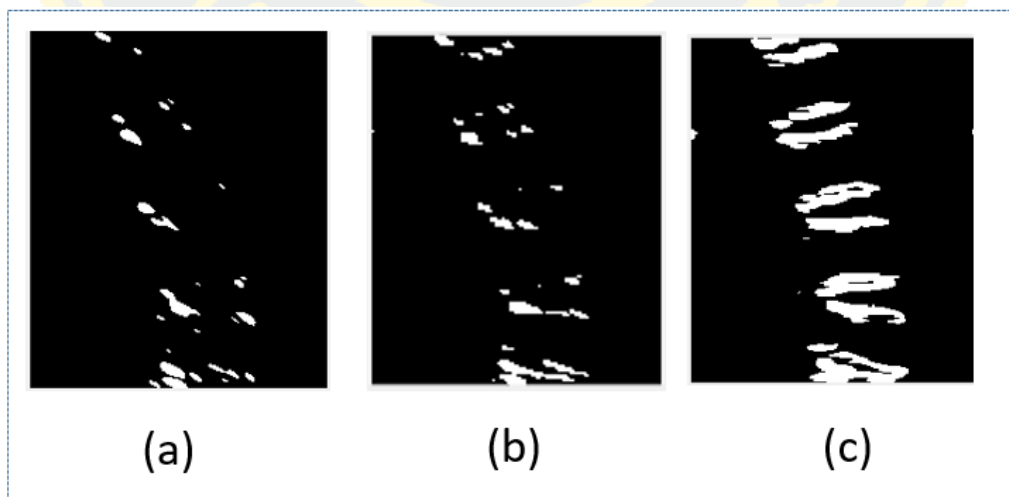


Figure 16 Example of applying Gabor filter to original grayscale image(a), output of Gabor filtering with $\theta = 0$ (b) and output of Gabor filter with $\theta = 90$ (c)

As shown in Fig.8 (a) and Fig.8 (b), output image of Gabor filter with $\theta = 60$ and $\theta = 90$ reveals only few parts of interested objects. So that, Output images of Gabor filter in range of $\theta = 60$ and $\theta = 120$ are merged into one output image as demonstrate in Fig. 7 (c) and can be defined as Eq. 11

$$I_{mgb}(\theta_1, \theta_2) = \sum_{i=\theta_1}^{\theta_2-1} \{I_{gb}(i) \cup I_{gb}(i+1)\} \quad (15)$$

Let I_{mgb} is an output image of Multi-theta Orientation Gabor filter. θ_1, θ_2 are the initial and final theta of Gabor filter function respectively and I_{gb} is an output of Gabor filter function as described in Eq. 15

```

Algorithm Gabor Filtering


---


Input :  sigma, theta, lambda, psi, gamma
Output : gb (Gabor Filter)
Begin
1:  sigma_x = sigma
2:  sigma_y = sigma/gamma
3:  nstds = 3
4:  xmax = max(abs(nstds*sigma_x*cos(theta)),
              abs(nstds*sigma_y*sin(theta)))
5:  xmax = ceil(max(1, xmax))
6:  ymax = max(abs(nstds*sigma_x*sin(theta)),
              abs(nstds*sigma_y*cos(theta)))
7:  ymax = ceil(max(1, ymax))
8:  xmin = -xmax; ymin = -ymax
9:  [x, y] = meshgrid(xmin:xmax, ymin:ymax)
10: x_theta = x*cos(theta)+y*sin(theta)
11: y_theta = -x*sin(theta)+y*cos(theta)
End

```

Figure 17 Gabor filtering Method

```



---


Algorithm Multi-theta orientation Gabor Filtering


---


Input :  initTheta, stopTheta, step, img
Output : output img
Begin
1:  For i = initTheta : step : stopTheta
2:      Bw = gabor_filter(img, i)
3:      Output_img = merge(output_img, bw)
4:  endfor
End

```

Figure 18 Multi-theta Gabor filtering Method

Then, opening image morphology is used to remove insignificantly small objects in the binary output image from multi-theta orientation

Gabor filter. Opening image morphological can be described in Eq. 4. The output of noise removing using opening image morphological is shown below:

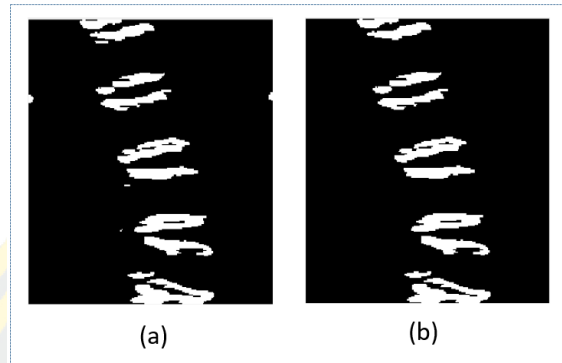


Figure 19 Output from multi-theta Gabor Filtering (a) and Noise removed image (b)

3.2.3 Geometric-Ellipse Shape Analysis

From observation, Shape of human lumbar vertebrae pose looks similar to ellipse shape as shown in Figure20

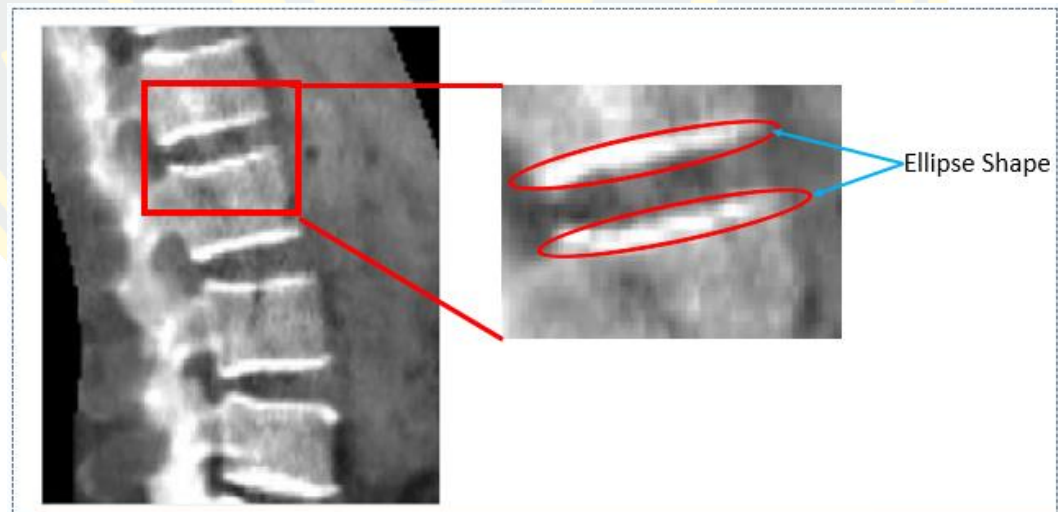


Figure 20 Ellipse-Shape like of human vertebrae pose

After removed small objects, Geometric Ellipse is applied to analyze the shape of vertebrae pose. Once the objects in the image are labelled, ellipse shape objects are generated using a point in center of each objects as a center point of each one ellipse. The proposed method used ellipse analysis to differentiate among different patterns of bone

structure. By using Principal Component Analysis (PCA), the major axis, minor axis and orientation of each objects are calculated. The first component and the second component of each objects are become an Ellipse major axis and minor axis respectively as demonstrated in Figure21

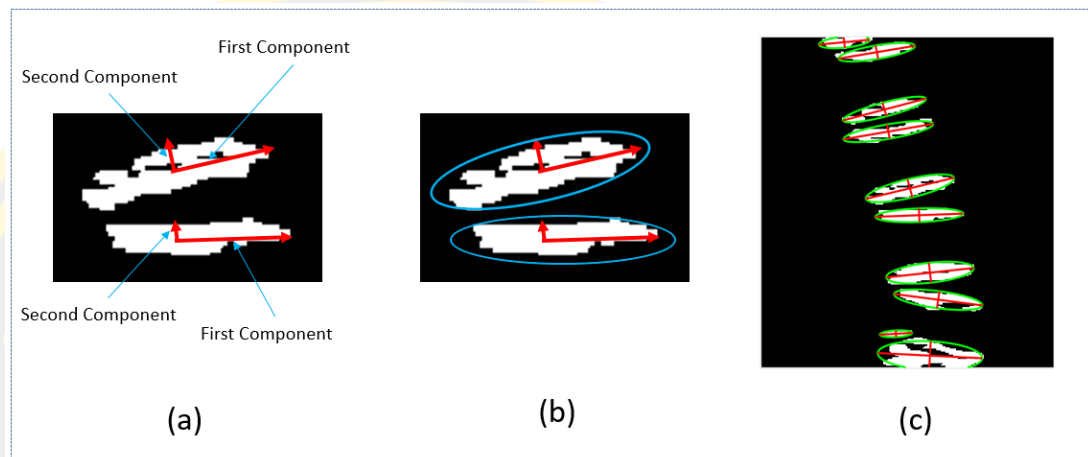


Figure 21 The first and second component of each objects (a), Apply an ellipse shape using the first and the second components (b), all ellipse with major axis and minor axis.

After selected candidates, the left and right boundary of each vertebrae pose are estimated using polynomial with degree of three are employed as shown in Fig.21 (a). Curve fitting can be defined as below:

$$P(x) = P_1x^n + P_2x^{n-1} + \dots + P_nx^n + P_{n+1} \quad (16)$$

$$y = P_1x^n + P_2x^{n-1} + \dots + P_nx^n + P_{n+1} \quad (17)$$

Where $P(x)$ is the coefficient, y is the value of a polynomial, n is the degree of polynomial. In this research, a degree is equal to 3. This is because the spine structure have a curved like shape. The coordinates of each ellipse's major axis right and left are used to fit the curve. Then, vertebrae pose are estimated as shown in Fig. 22 (c)

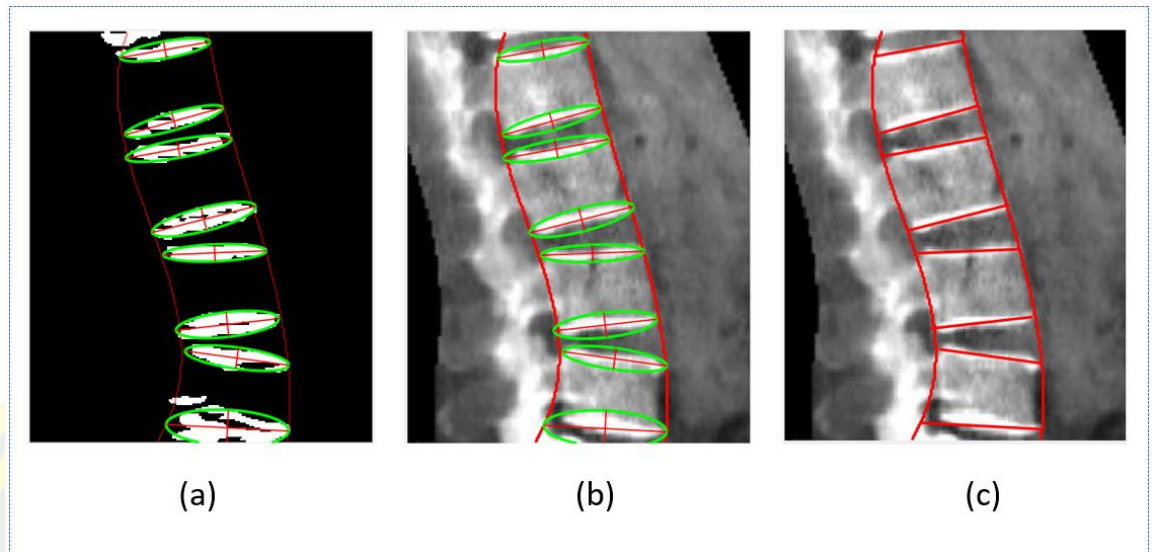


Figure 22 Selected candidates and vertebrae boundary estimation using curve fitting in binary image (a), Selected candidates and vertebrae boundary estimation using curve fitting in grayscale image (b), final output of vertebrae pose estimation (c)

3.2.4 Anterior-Posterior (AP) View lumbar vertebrae pose estimation

Each vertebrae pose was manually define by hand.

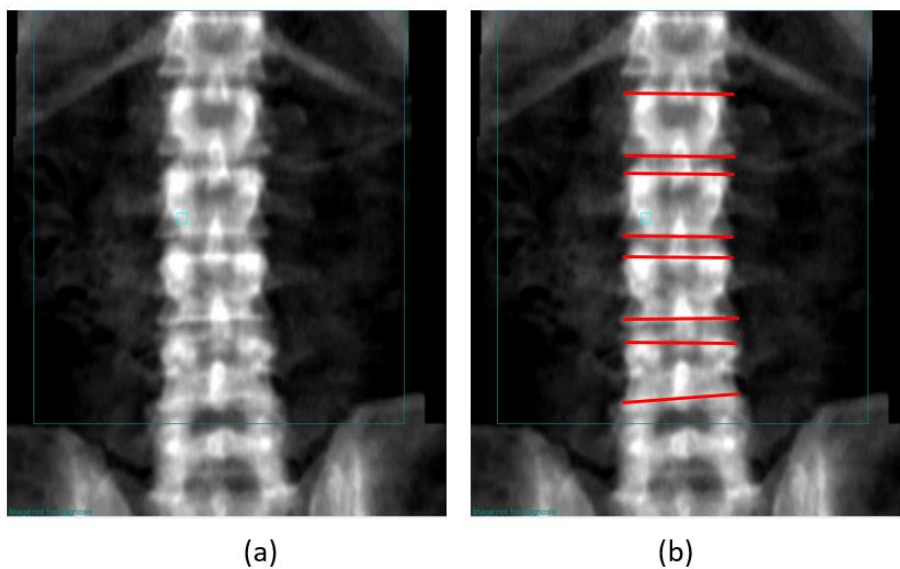


Figure 23 Original AP view (a) and Manually Vertebrae Pose Identification (b)

3.3 Three-dimensional Model Deformation

This phase is separated in 2 steps, consist of registration and deformation. In the registration step, estimated vertebrae pose of both view of lumbar are registered for determination of each pose position and angle. In the deformation step, the three-dimensional model template is read for deformation using the information from registration step.

3.3.1 Registration

To deform a three-dimensional model from 2 two dimensional image (Raster), the same point of each image must be mapped. It's called image registration. In this stage, the vertebrae pose which estimated from the former step (both view AP and Lateral view) are used to register the Lateral view to AP view. The estimated vertebrae pose is shown below:

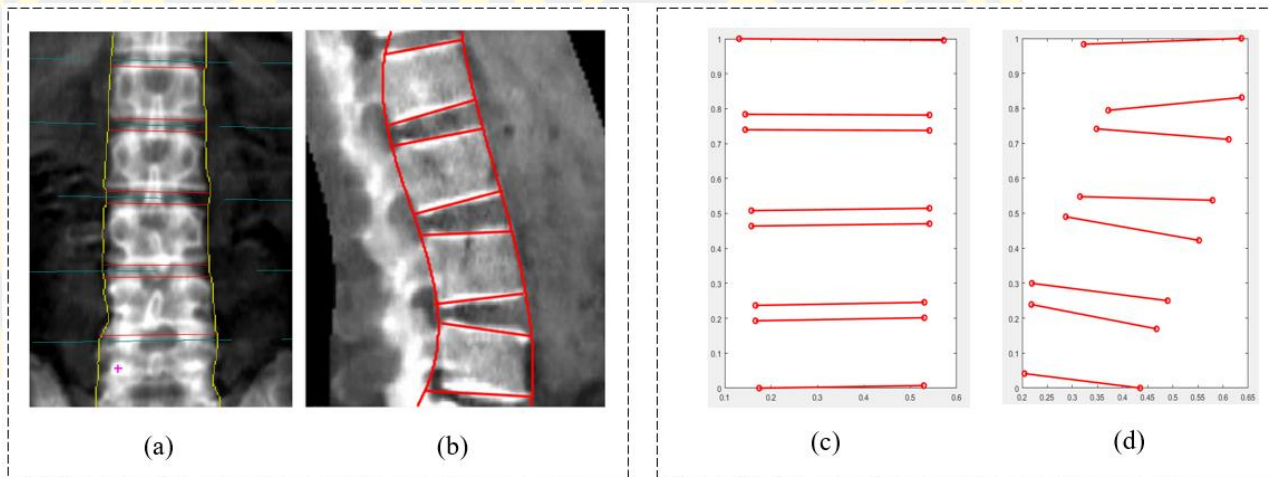


Figure 24 AP Side vertebrae pose identification manually (a), Lateral side vertebrae identification (b), normalized position of AP Side, and Normalized of lateral side (d)

Vertebrae pose which estimated in the former step is has a different dimension and scale. Therefore, those vertebrae poses are normalized to range of 0 and 1 [0, 1]. After that, the vertebrae poses are registered to each other. The normalization equation is demonstrated below:

$$X_{norm} = \frac{X - X_{min}}{X_{max} - X_{min}} \quad (18)$$

Where X_{norm} is a normalized data, X is an original data, X_{min} is a minimum value of all X and X_{max} is a maximum value of all X

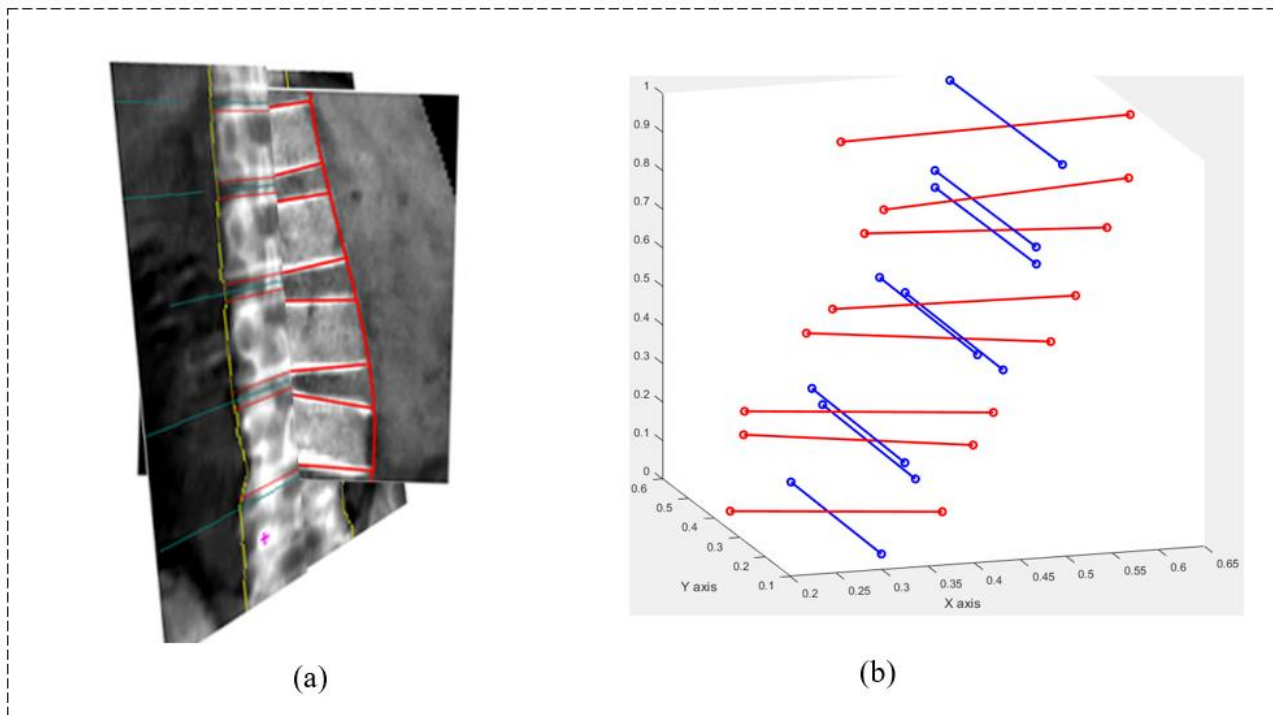


Figure 25 Registration of AP Side and Lateral Side

3.3.2 Deformation

In this step, the three-dimensional model template of human vertebrae is used to deform a model of human lumbar vertebrae from L1 to L4.. The template file contains vertices and polygon-faces of lumbar shape in three-dimension space. Then, the surface of the model has been created as show in Figure25.

9

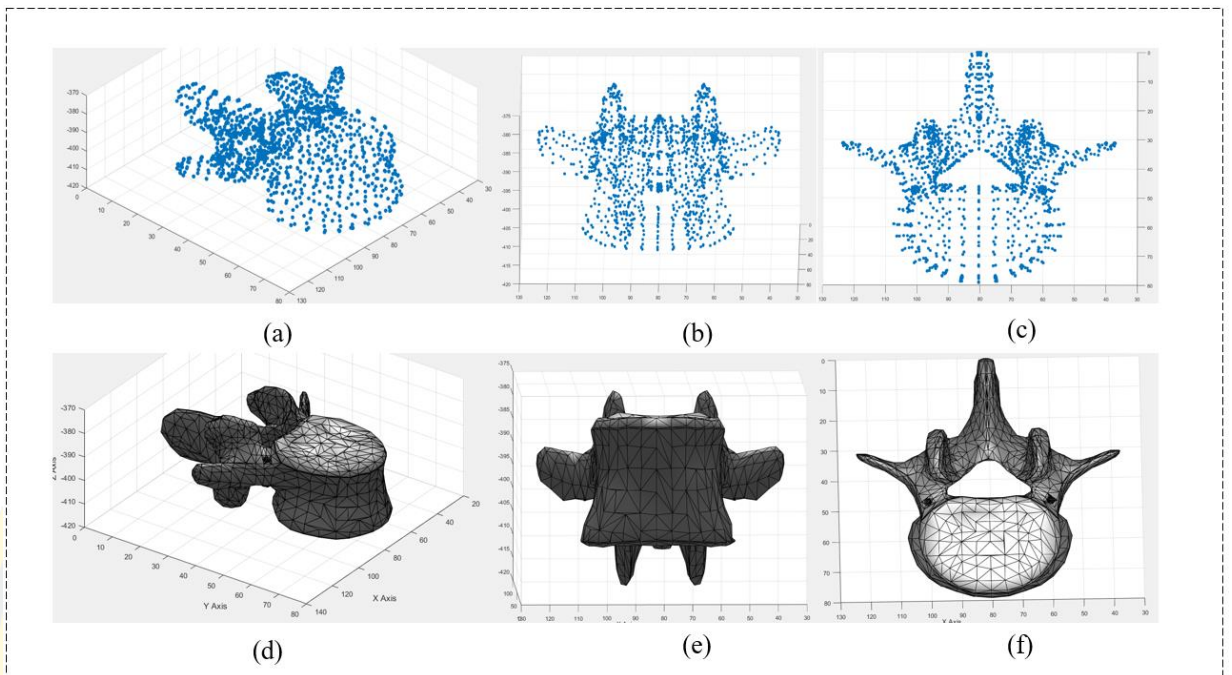


Figure 26 Imported template as scatter plot (a) (b) and (c), surface plotted template (d), (e) and (f)

The structure of imported template file is show below

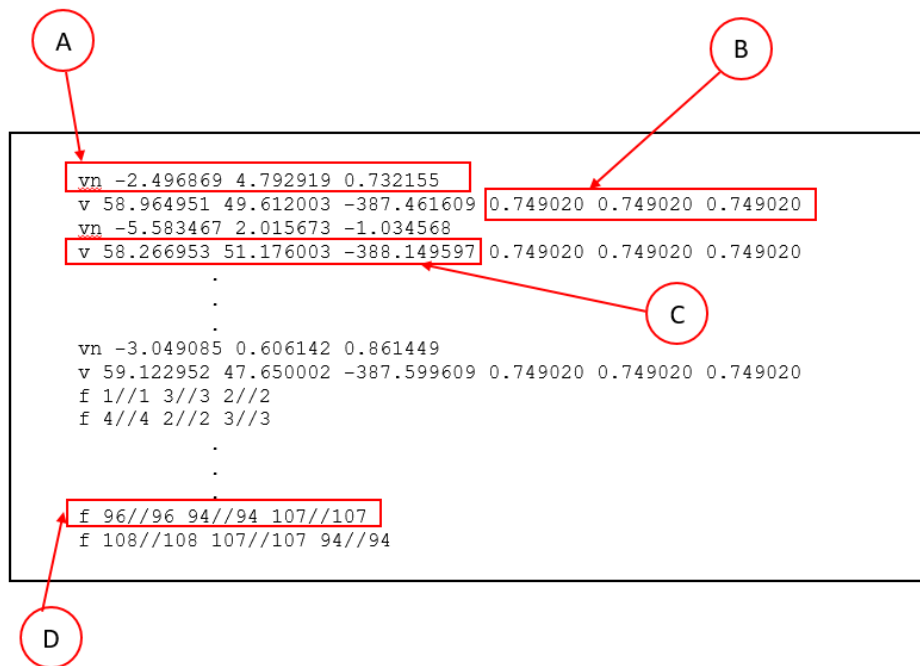


Figure 27 List of vertex normal (A), List of alpha value default to 1.0 (B), List of geometric vertices (C), and Polygonal face element (F)

OBJ file is a geometry definition file format first developed by Wavefront Technologies for its Advanced Visualizer animation package. The file format is open and has been adopted by other 3D graphics application vendors. The OBJ file format is a simple data-format that represents 3D geometry alone — namely, the position of each vertex, the UV position of each texture coordinate vertex, vertex normals, and the faces that make each polygon defined as a list of vertices, and texture vertices. Vertices are stored in a counter-clockwise order by default, making explicit declaration of face normals unnecessary. OBJ coordinates have no units, but OBJ files can contain scale information in a human readable comment line. After the template was imported, the construction of Lumbar vertebrae was constructed as shown in Figure28.

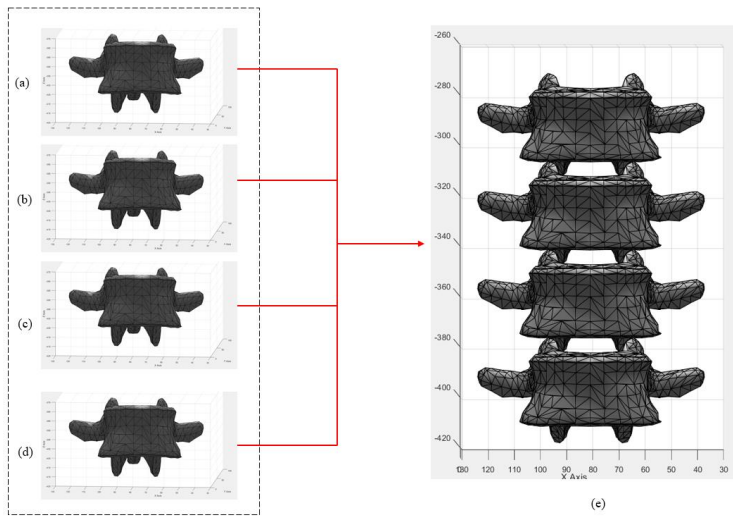


Figure 28 Construction of Human spine from imported template

After spine was constructed, each vertebrae is rotated. The angles of rotational were obtained from registration step.

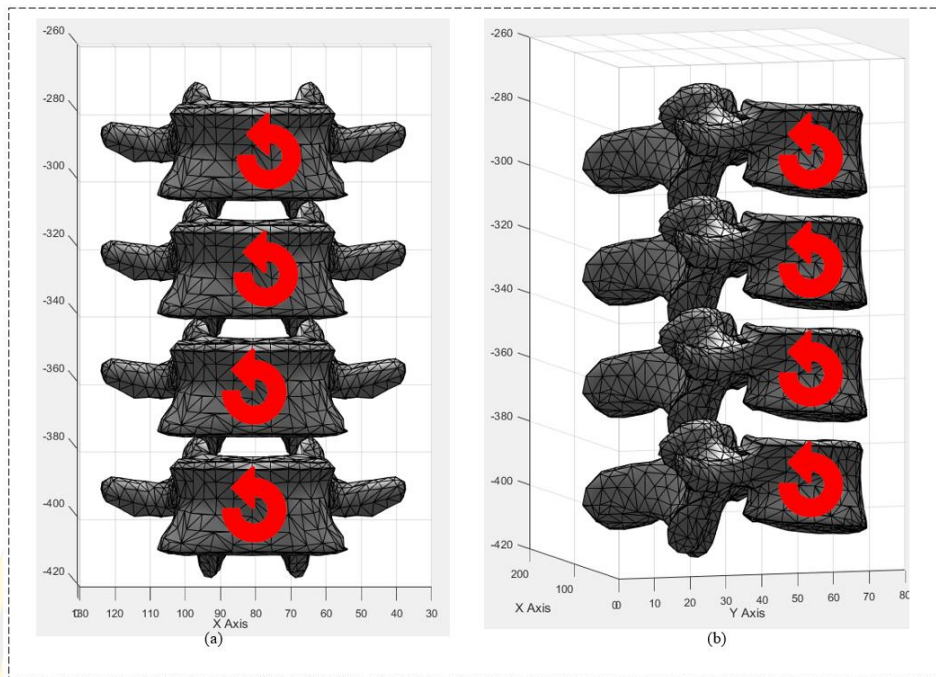


Figure 29 Rotation of each vertebrae

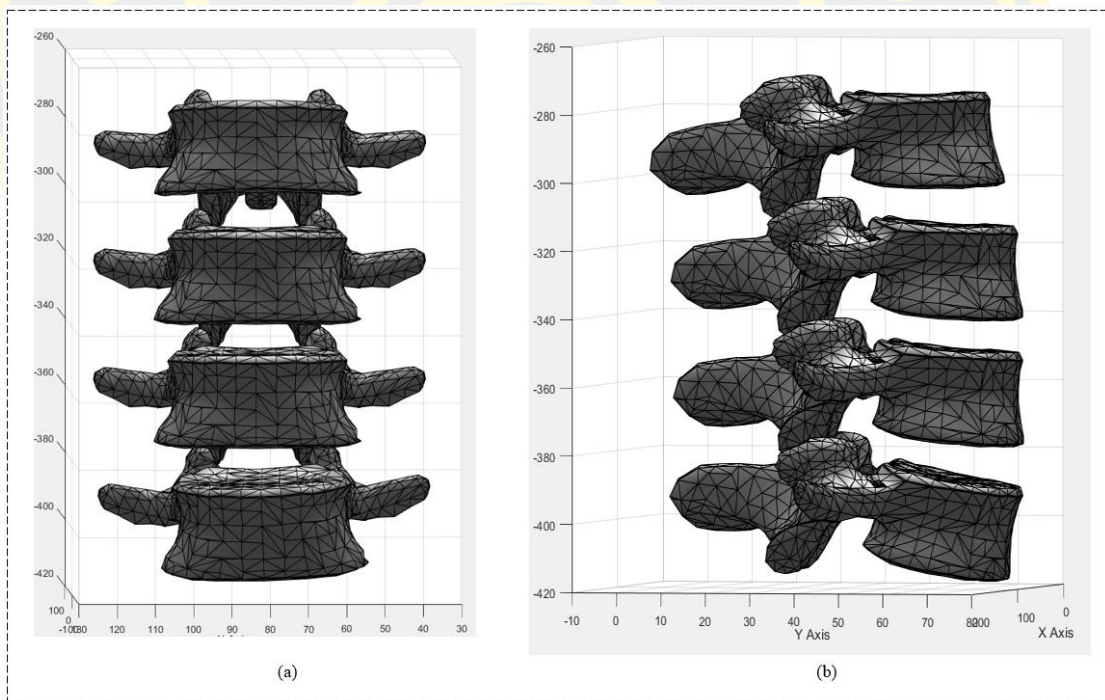


Figure 30 Result from rotational of each model

CHAPTER 4

EXPERIMENTAL RESULTS

From research methodology as described in Chapter 3, it consists of three main phases. In the first phase, to evaluate the efficiency of the proposed algorithms, 70 spine X-ray images obtained from DXA (dual-energy X-ray absorptiometry) scanning machine authorized by Burapha University Hospital are employed. The dataset contains three levels of X-ray radiation values including low, medium, and high radiations. Each radiation value level provides different image quality. On the other hand, low radiation level produces low quality image. Then, the experimental results were compared with the ground-truth images obtained by radiologists of Burapha University Hospital.

4.1 Region of Interest Segmentation

In this step, the main idea of this proposed method is to segment necessary regions of interest on the given image. To identify or estimate the vertebrae pose of lumbar region in the next phase must eliminate other region. As known that the low radiation image contains a number of noises, then it makes difficulty in detecting the boundary of the object image. Then, some image pre-processing algorithms have been used in order to improve quality of the input image as follow:

4.1.1 Binarization using Image Entropy value

Input image is disturbed from undesired object. So that, the hypothesis of this step is the entropy value can separate desired object from undesired object. Then, input image is binarized using Entropy value. The lumbar area is seem to disappear because the vertebrae body of this area is quite narrow as show in Fig. Then, small objects were remove using connected-component labeling. Small components are removed as shown in **Fig**

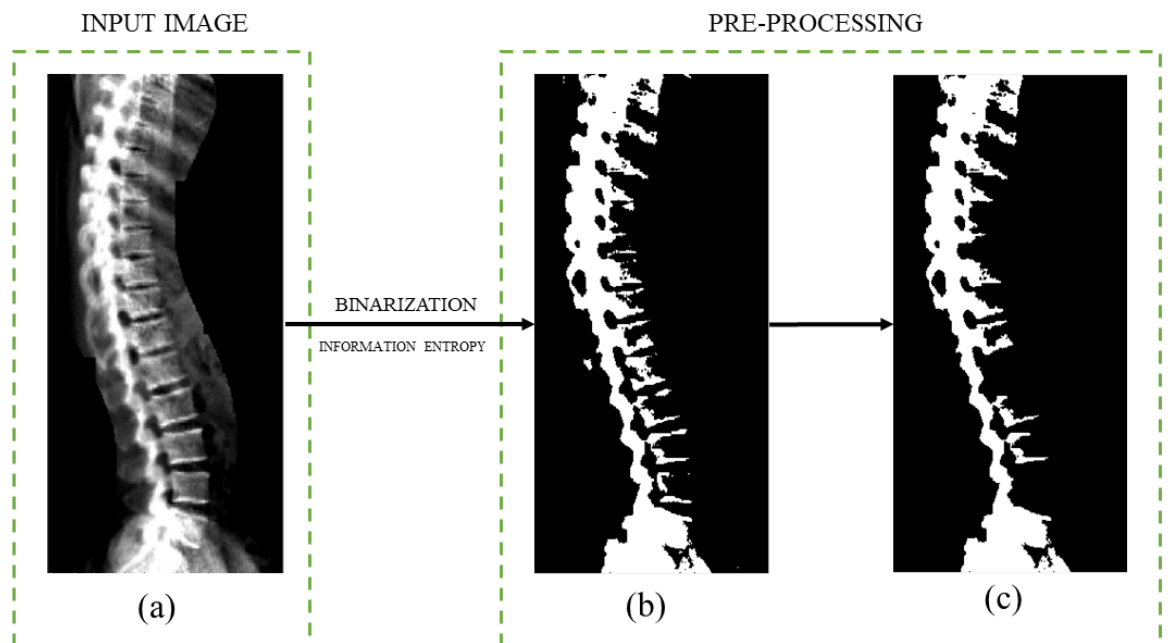


Figure 31 Original Input (a), output of binarization (b), and result of small object removing (c)

4.1.2 Horizontal Projection

In this stage, horizontal projection is performed to reveal a pattern in one-dimensional space as demonstrated in Figure 31. From Observation, the region which seem to be a lumbar region is like an abyss in the horizontal projection graph. So that, this area will be identified in the up coming step.

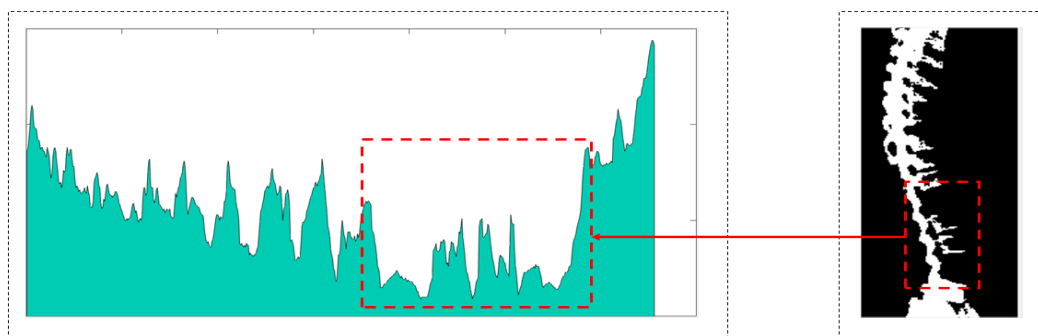


Figure 32 Result of horizontal projection

After horizontal projection is applied, the graph is smoothen to reduce complexity of information and to reduce insignificant peaks point. The result of local maxima finding is shown below:

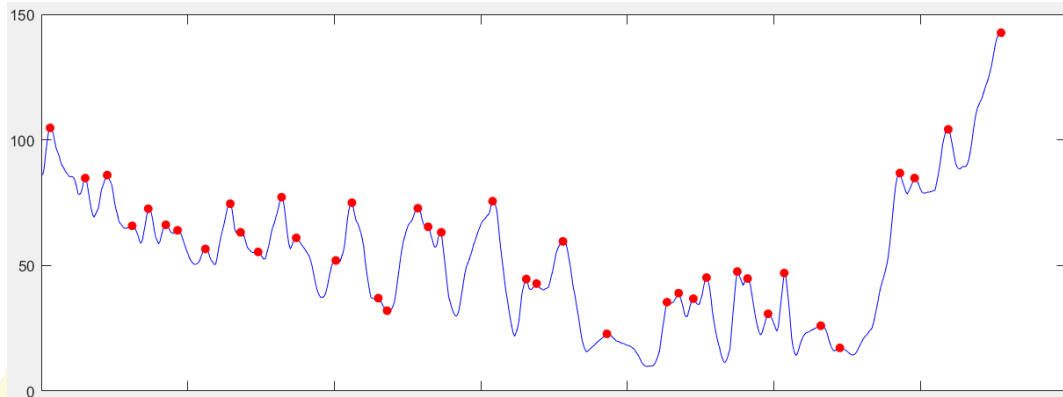


Figure 33 Result of local peaks finding

4.1.2 Triangular Analysis

From chapter 3, Triangular analysis is used to determine the upper boundary and lower boundary of lumbar region. Firstly, triangles are drawn from adjacent peaks point as shown in Figure33. Candidates are selected. Finally, the boundary of upper boundary and lower boundary are determined as shown in Figure33.

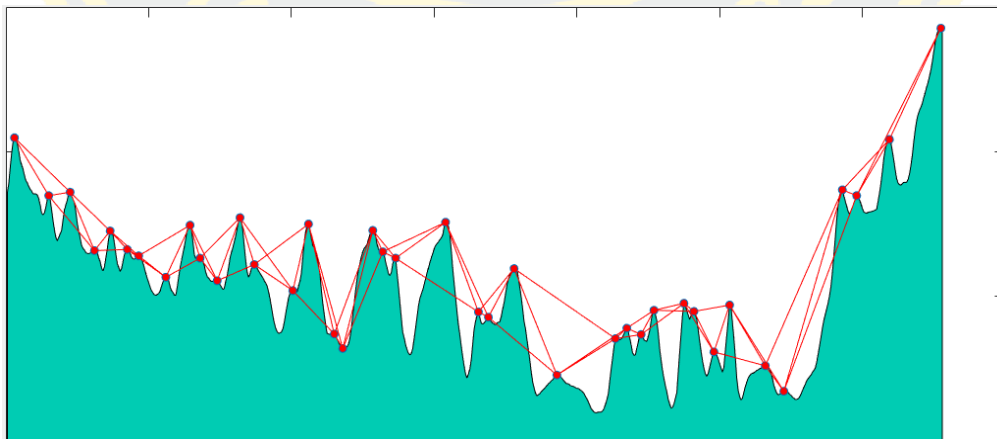
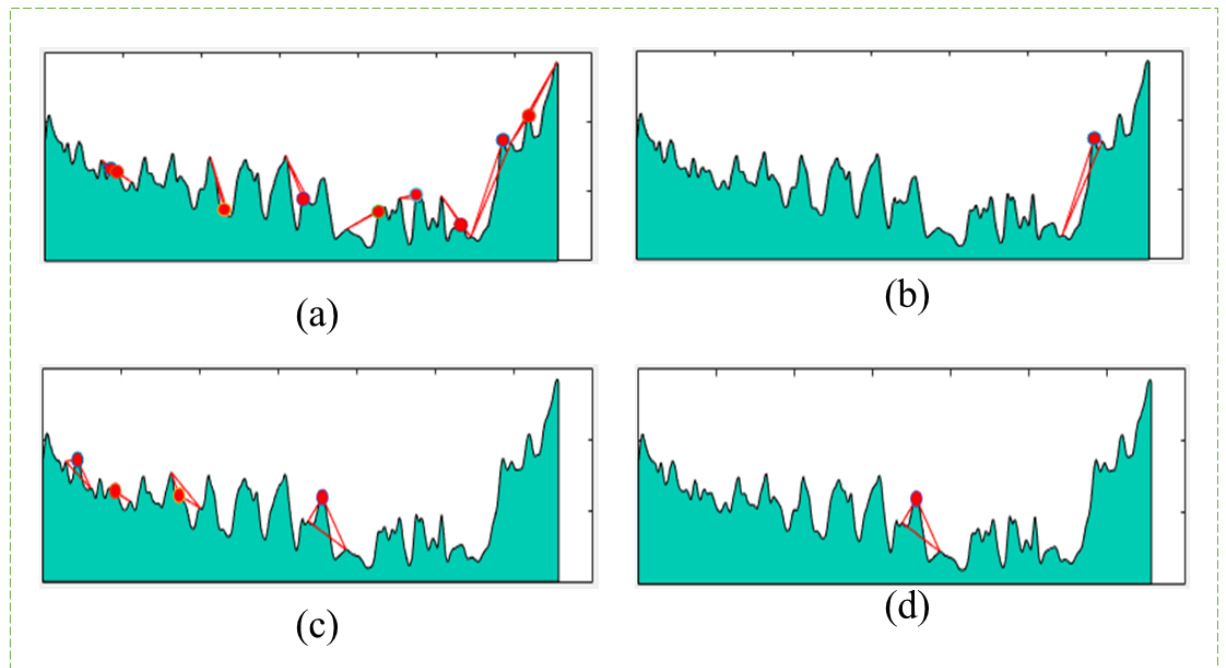


Figure 34 Result of triangular drawing on each local peaks



After those boundary are determined, the region of lumbar spine is segment from whole spine image as shown below:

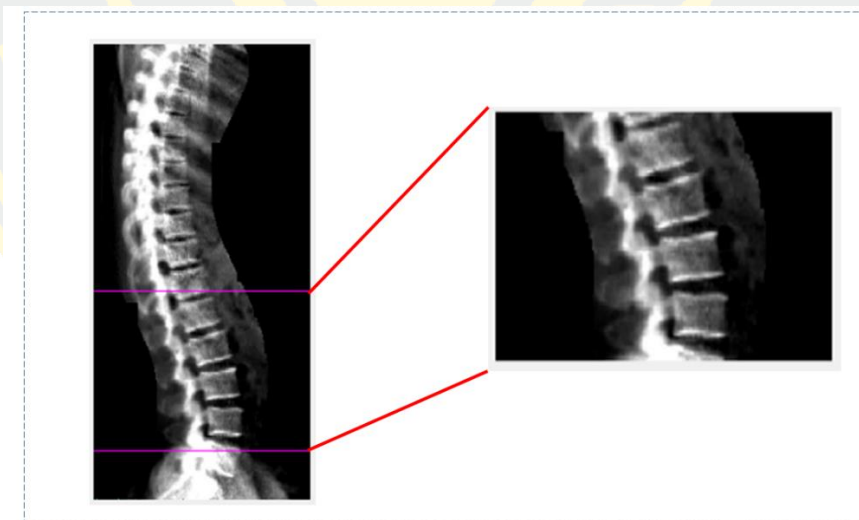


Figure 35 Final result of Region of interest segmentation

The efficiency of the proposed method is validated by using overlap region techniques between the proposed method and ground-truth. Thus, the efficiency of this section is evaluated by using Jaccard index and Area Overlap (AO) to compare the similarities between two algorithms and

ground truth image. The Jaccard index and Area Overlap (AO) were defined as equation (4-1), and (4-2). Then, In Table 3 and 4 were shown that the performance measurement using Jaccard index and Area Overlap (AO) coefficient. Finally, in table 5 and 6 were concluded of the percentage information from each algorithm.

$$J(A, B) = \frac{|A \cap B|}{|A \cup B|} \quad (19)$$

where A = ground-truth image, B = segmented image.

$$A = \frac{|IM_1 \cap IM_2|}{|IM_1 \cup IM_2|} \times 100 \quad (20)$$

where IM = image which want to compare.

Table 2 Percentage of Jaccard index and AO

Image	Pure Vertical Projection		Triangular Analysis	
	Jaccard index	Area Overlap	Jaccard index	Area Overlap
1	45.36	31.53	88.15	88.09
2	77.79	79.12	83.08	84.22
3	88.68	83.41	63.42	60.16
4	72.48	73.64	83.71	84.81
5	79.84	81.14	77.54	80.67
6	82.52	83.45	84.70	85.24
7	83.61	84.44	83.44	84.46
8	55.02	63.16	83.42	85.15
9	77.72	80.16	77.20	80.02
10	82.26	82.64	80.20	82.21
.				

.				
.				
65	84.09	84.38	83.66	83.99
66	87.70	86.91	83.06	84.56
67	73.78	75.49	83.37	84.66
68	82.31	83.12	78.98	80.92
69	58.40	68.02	81.43	83.40
70	79.64	78.49	84.71	84.24

Table 3 Conclusion of percentage of Jaccard index and Area Overlap

	Pure Vertical Projection		Triangular Analysis	
	Jaccard index	Area Overlap	Jaccard index	Area Overlap
Least	45.36	31.53	54.15	57.09
Most	77.79	79.12	83.08	84.22
Average	62.68	55.41	71.42	75.16

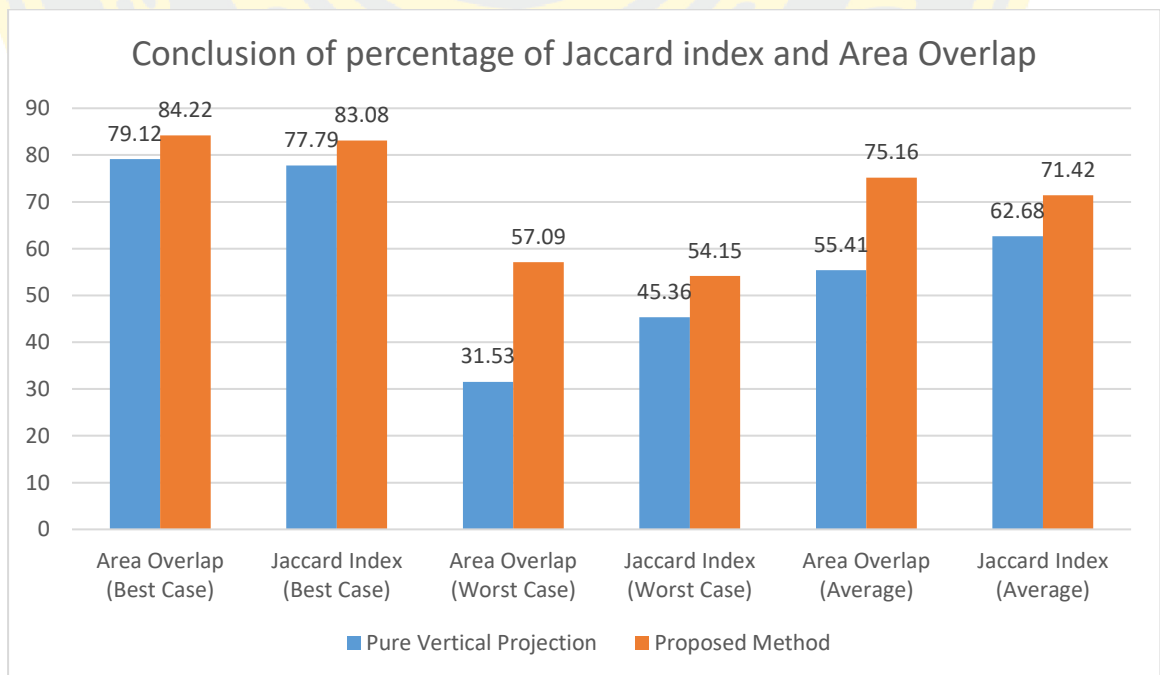


Figure 36 Comparison of evaluation

In the proposed method, the dataset which contained 100 low radiation lateral-side lumbar vertebrae images were collected from local hospital. The images produced from Dual-Energy X-ray Absorptiometry (DEXA) consist of low quality, medium quality and high quality image. The experimental result is compared with ground-truth which provided by experts radiologist from local hospital. The efficient was evaluated by using confusion matrix. The result is shown in Table 4.

Table 4 Percentage of True Positive (TP), False Negative (FN), False Positive (FP), and True Negative (TN) using Eduardo A. Ribeiro's method.

Image	TP	FN	TN	FP
1	0	0	1	0
2	0	0	0	1
3	0	0	1	0
4	0	0	1	0
5	0	0	0	1
6	0	0	0	1
7	0	0	1	0
8	0	0	1	0
9	0	0	1	0
10	0	0	0	1
11	0	0	0	1
12	1	0	1	0
13	1	0	0	1
14	0	0	0	1
15	0	0	0	1
16	0	0	1	0
17	1	0	1	0

18	0	0	0	1
19	0	0	0	1
.				
.				
.				
63	1	0	0	0
64	1	0	0	0
65	1	0	0	0
66	1	0	0	0
67	0	1	0	0
68	1	0	0	0
69	0	1	0	0
70	0	1	0	0

4.2 Lateral Vertebrae Pose Estimation

In the proposed method, the dataset which contained 70 low radiation lateral-side lumbar vertebrae images were collected from local hospital. The images produced from Dual-Energy X-ray Absorptiometry (DEXA) consist of low quality, medium quality and high quality image. The experimental result is compared with ground-truth which provided by experts radiologist from local hospital. The efficient was evaluated by using confusion matrix. The result is shown in Table 5.

Table 5 Percentage of True Positive (TP), False Negative (FN), False Positive (FP), and True Negative (TN) using proposed method.

Image	TP	FN	TN	FP
1	0	0	1	0
2	0	0	0	1

3	0	0	1	0
4	0	0	1	0
5	0	0	0	1
6	0	0	0	1
7	0	0	1	0
8	0	0	1	0
9	0	0	1	0
10	0	0	1	0
.				
.				
.				
65	1	0	0	0
66	1	0	0	0
67	0	1	0	0
68	1	0	0	0
69	0	1	0	0
60	0	1	0	0

Table 6 Performance Measurement Result

Measurement	Eduardo's	Proposed Method
Accuracy	40.00%	61.25%
Sensitivity	40.90%	50.00%
Specificity	39.65%	65.51%

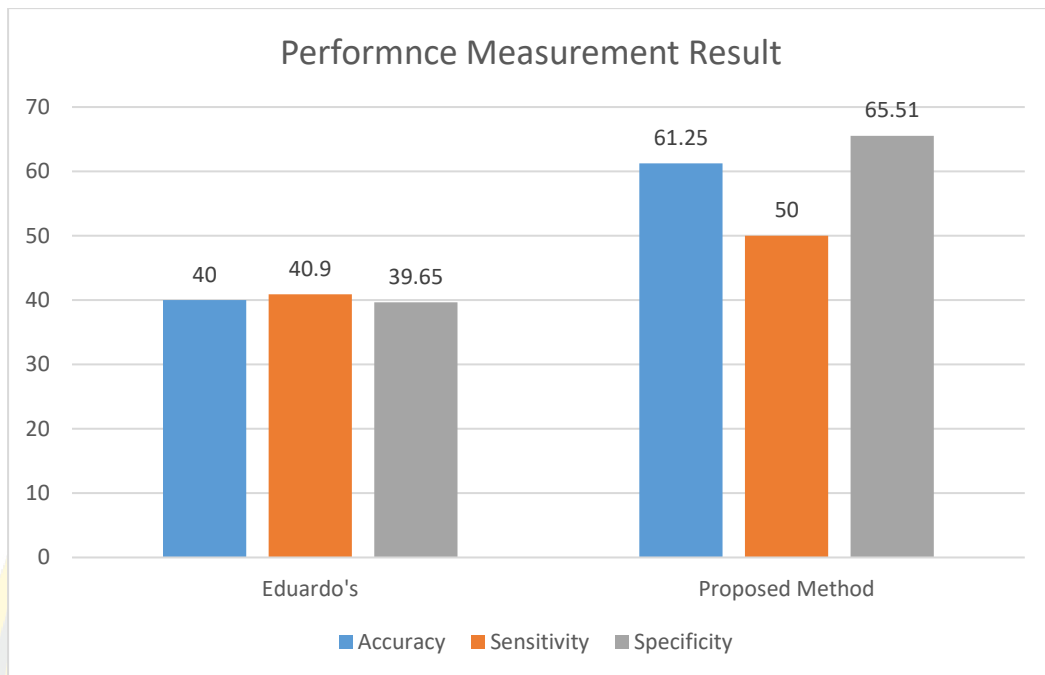


Figure 37 Comparison of vertebrae pose segmentation's result

4.3 Three-Dimensional Deformation

In this step, the results from deformation process were validated with three-dimensional model ground-truth as shown in Figure 37 (a). The results in table 7 were computed using Mean Squared Error (MSE) of each deformed vertebrae and ground-truth model. MSE can be described as below:

$$MSE = \frac{1}{n} \sum_{i=1}^n (A_i - B_i)^2 \quad (21)$$

Where n is a number of vertices in each model, A_i is a vertex of model A and B_i is a vertex of model B.

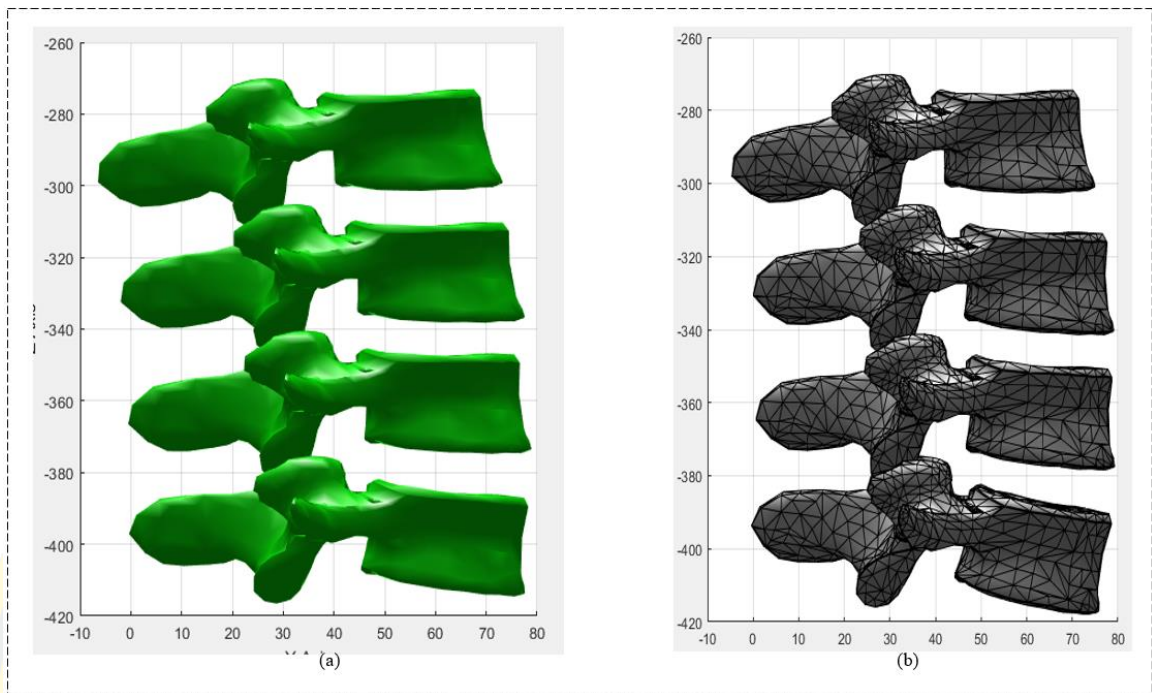


Figure 38 Ground-truth model (a) and result of proposed method (b)

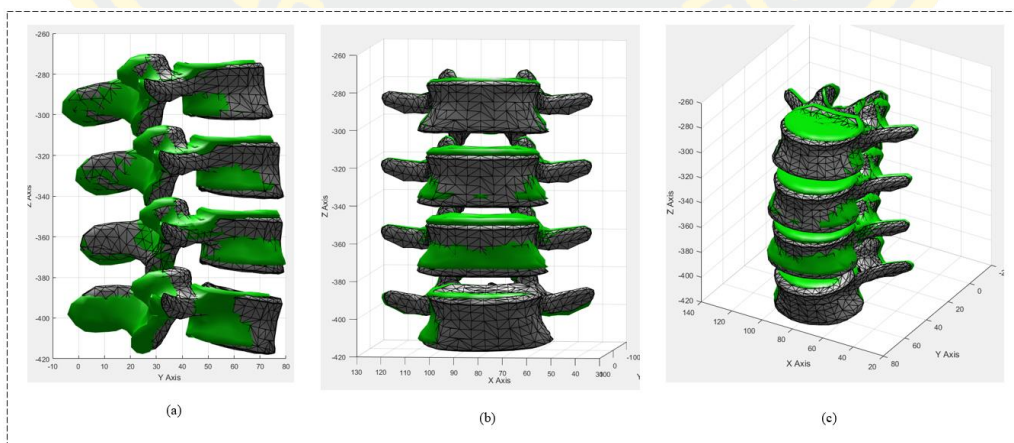
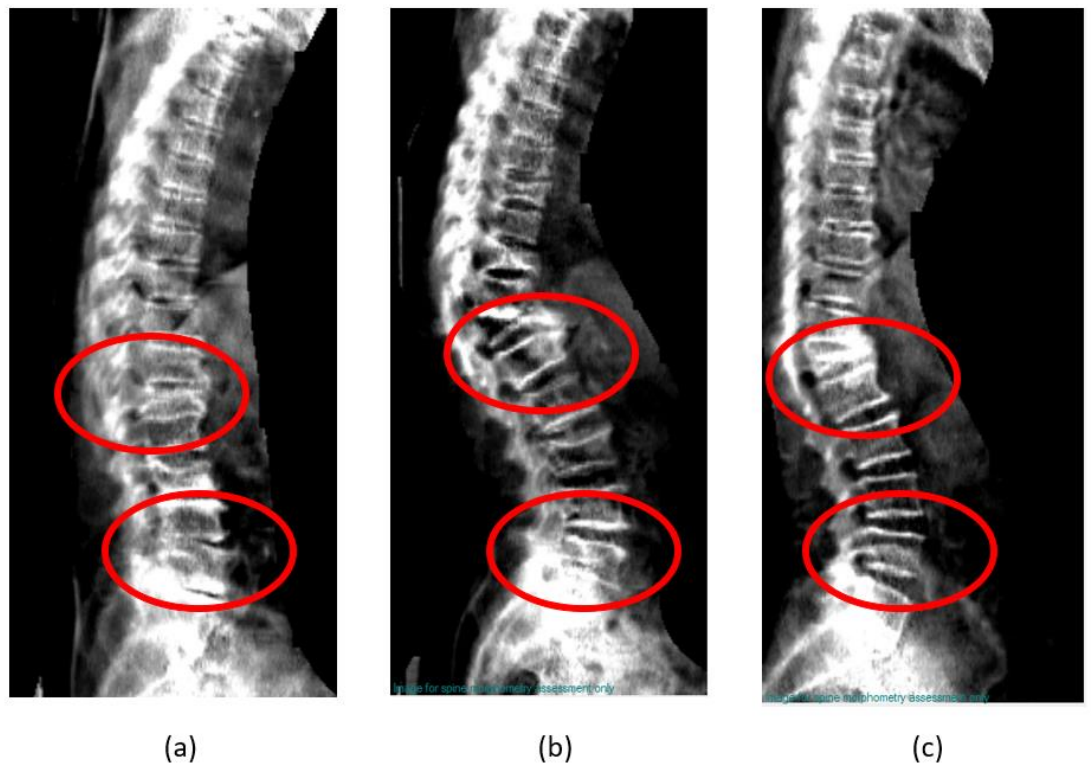


Figure 39 Volume overlap evaluation of proposed model and ground-truth

Table 7 Mean Square Error (MSE) of Deformed Model compared with model ground-truth using proposed method.

Image	L1	L2	L3	L4
1	1.32	1.52	1.10	3.51
2	3.29	0.43	6.83	2.75
3	0.68	0.32	0.55	0.36
4	0.98	0.58	0.32	0.67
5	5.37	0.81	0.11	1.41
6	5.89	1.35	1.32	2.31
7	0.81	0.92	2.12	2.01
8	4.35	0.61	0.45	3.12
9	11.5	0.12	0.65	1.21
10	6.44	1.02	0.45	4.15
.				
.				
.				
65	7.08	1.76	1.78	0.55
66	6.61	1.81	1.97	3.33
67	4.23	1.65	0.07	1.25
68	2.24	0.24	1.87	4.25
69	4.1	0.68	1.84	0.92
70	5.99	0.5	0.9	5.39

The result reveal that L1 and L4 vertebral is gain a huge errors. Because of the information from vertebrae pose estimation step, L1 and L4 are located on a very low contrast area and disturbed with obstacles such as Sacrum bone which is near L1 vertebrae as shown in Figure40.



In Figure40 (a), it show up a noise from ribs and some bone lesion which increases the error in the propose method.

CHAPTER 5

CONCLUSION AND DISCUSSION

5.1 Conclusion

In this study, a methodology for three-dimensional deformation of lumbar vertebral bone body on low radiation image. The proposed methodology consists of three main phases. In the first phase a methodology for segmenting boundary of the lumbar vertebral body image is performed. In the second phase, lumbar vertebrae poses are estimated. In the last phase, a three-dimensional model of lumbar vertebrae is deformed.

In the first phase, a new method using triangular analysis for lumbar segmentation from low-radiation radiography image produced from Dual-energy X-ray Absorptiometry is proposed. The proposed method consists of three main steps. Firstly, the pre-processing step consists of binarization and morphological techniques. These techniques are applied to remove background and noises. Secondly, the output from step one is transformed into horizontal projection. The output of horizontal projection is then used to find local maxima which located the peak points. Triangular shape is formed using a peak with its left and right adjacent peaks. Finally, candidate objects are determined using proposed features of the triangular shape. The proposed method can automatically locate the region of human lumbar spine. This can help to reduce work load of radiologist. In general, the proposed method can be used as a preprocess for other research in the area of bone structure identification and segmentation

In the second phase, research proposed the method to automatically estimate vertebrae pose in low-radiation X-ray image. The datasets were produced from Dual-Energy X-ray Absorptiometry (DEXA) from local hospital. By using Modified Gabor filter combining with geometric ellipse shape analysis, the vertebrae pose is estimated. The proposed method is divided in 3 main phases. In the first phase, the input image is enhanced using Top-Hat filtering. In the second phase, multi-theta orientation Gabor filter is used to extract vertebrae pose candidates. Then, all connected-component candidates are labeled for removing all small

candidates. In the final phase, Principle Component Analysis (PCA) and Ellipsoidal Analysis are used to determine orientation of each vertebrae pose. After that, lumbar spine line is estimated using polynomial curve fitting. The proposed method can automatically estimate the region of human lumbar vertebrae pose with 81.9% of accuracy, 90.07% of precision 88.5% of recall and 11.5% of false negative rate.

By using an information from two former phases and ground-truth AP side's information, the three-dimensional model of human lumbar vertebrae is deformed. In the last phase, the methodology is separated in three steps. Firstly, a three-dimensional model of vertebrae is imported. Then, we will iterate the model for four items (L1, L2, L3 and L4 lumbar vertebrae). After that, the estimated vertebrae poses are used to rotate each vertebrae to the same degree as each pose. The results are compared with ground-truth which provided by the experts.

5.2 Contributions

The result of three-dimensional model from the methodology can be used for a variety of purposes, including biomedical modelling for orthopaedics (Barbieri, Pedrosa, Traina, & Nogueira-Barbosa, 2015) or anatomical applications. To facilitate better surgical results in rheumatoid cervical spine. Generally, in Three-Dimensional model Deformation and reconstruction must be done by using an expensive machine or a very high dose of radiation. So that, the patients are gaining risks from those machine. Exposing a high dose of radiation, increases many risks of genetic distorted diseases such as cancer or abnormally gene etc. According to the report, patients absorb 25 – 360 mSv (milli-Sievert) per one time that Computational Thermography Scanner is operated. Normally, human absorbs radioactive for 1.5 mSv per one year in natural. It means that, the patients absorb a radioactive twenty years more when compare to natural absorption.

5.3 Discussion

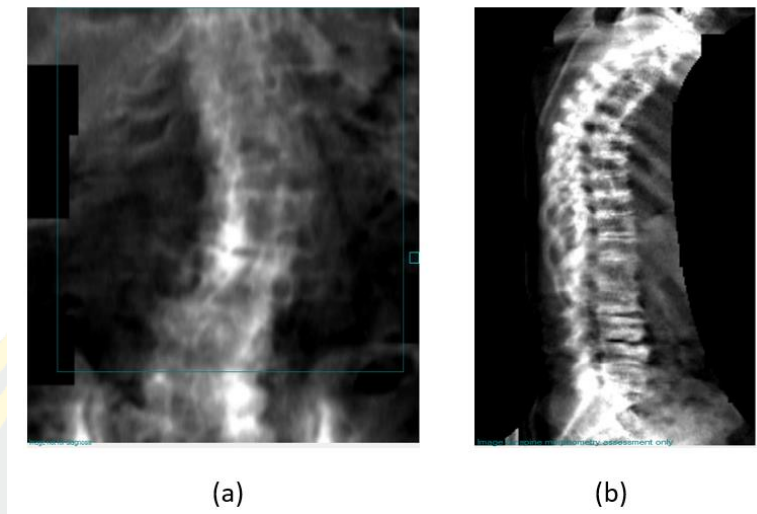


Figure 40 Example of Bone Collapse case in AP view (a) and Lateral view (b)

In the first phase, the proposed method can be used as a preprocessing for other research in the area of bone structure identification and segmentation. In future work, the segmentation of lumbar region for special cases of exostosis and bone collapse is going to be attempted. In the second phase, the proposed method also cannot work in the dataset with high-level damaged vertebrae pose from lesion of exostosis and bone collapse. So that, the result in the final step will not work in those cases.

5.3 Future Work

- The segmentation of lumbar region for special cases of exostosis and bone collapse is going to be attempted.
- Followed-up of Three-dimensional model of consecutive human lumbar spine will be deformed.



ETHICS





PUBLICATIONS



ORGANIZING COMMITTEE

Advisory Committee

- Masaru Niikawa (Osaka University, Sweden)
- Wenwu Lu (Nanyang University, Japan)
- Arking Song (Shanghai University, Republic of Korea)
- Zou Cheng (Nanyang Technological University, Singapore)
- Wu Jian (Nanyang Technological University, Singapore)
- Masashi Tsunoda (Osaka University, Japan)
- Wang Guany (Kobe University, Japan)

Honorary Chair

Shin-ichi Ochiai (Nagoya University, Japan)

General Chair

- Kaew-Chanongphol (King Mongkut's University of Technology Thonburi, Thailand)
- Yu-Kang Ho (Chungyang Institute of Science and Technology, Republic of Korea)
- Kiwi Horvath (Osaka University, Japan)
- Jing-Ming You (National Central University of Science and Technology, Taiwan)
- Feng-Lai Phiang (Technological University, Singapore)
- Chai Eun-Ho (Hankyong University, Malaysia)

Program Chair

- Suwan Inook (Chulalongkorn University, Thailand)
- Ferdinand (King Mongkut's University of Technology Thonburi, Thailand)
- Huan-Yu Liu (Universiti Teknikal AMBA Kelantan, Malaysia)
- Bongsoo Lee (Chungnam National University, Republic of Korea)
- Koh Kawamura (KDDI Research, Inc., Japan)
- Yun-Hong Lee (National Cheng-Chung University, Taiwan)
- Kumar Gnan (Nanyang Technological University, Singapore)
- Masaru Niikawa (Osaka University of Technology, Thailand, Thailand)

Publicity Chair

Jong-Hyeon Kim (Kangwon National University, Republic of Korea)

Special Session Chair

- Sung-Jin Lee (Shanghai University, Republic of Korea)
- Chun-Hong Tzeng (National Sun Yat-sen University, Taiwan)
- Sun-Chang Lu (Universiti Teknikal AMBA Kelantan, Malaysia)
- Nattapong Hanthaisri (Kangwon National University of Technology, Pochonng, Thailand)
- Tsunehiko Imai (Osaka University, Japan)

Local Arrangement Chair

Ekkanat Boonlathong (Chulalongkorn University, Thailand)

Somchai Chaiyapichit (King Mongkut's University of Technology Thonburi, Thailand)

Registration Chair

- Kasorn Chantavan (Rajabhat Mahasarakham University of Technology, Mahasarakham, Thailand)
- Wattana Kwanthak (King Mongkut's University of Technology Thonburi, Thailand)

Finance Chair

- Lekha Sangka (King Mongkut's University of Technology Thonburi, Thailand)
- Sudat Tansakul (King Mongkut's University of Technology Thonburi, Thailand)

Publisher Chair

Piya Wacharasindhu (Bangkok University, Thailand)

Secretary

Thiraporn Chansong (Chulalongkorn University, Thailand)

First Call-for-Papers

10th International Workshop on Advances Image Technology (IWAIT 2018) will be held on January 1-4, 2018 in Chiang Mai, Thailand. IWAIT 2018 will provide an international forum for researchers and engineers who are interested in the field of advanced image technologies.

TOPICS

IWAIT 2018 is going to cover advanced topics of image/video and multimedia technologies. The topics include, but not limited to:

- 2D/3D Image/Video Processing
- Pattern Recognition
- Image/Video Compression
- Video on Demand
- Broadbanding
- Networked Multimedia
- Multimedia Systems
- Big Data Image/Video Analysis
- Multimedia Applications
- Computer Vision
- Medical Imaging & Applications
- Virtual Reality
- Animation
- Computer Graphics
- Cloud Multimedia Computing
- Social Multimedia

PAPER SUBMISSIONS

Prospective authors are invited to submit their original papers in 2-4 pages including figures and tables in English. All papers are to be submitted electronically in the PDF format.

IMPORTANT DATES

Special session proposal	July 31, 2017
Extended abstract submission	August 31, 2017
Notification of acceptance	October 31, 2017
Submission of camera-ready full papers	November 4, 2017

Organized by:

- King Mongkut's University of Technology Thonburi, Thailand
- Center of Excellence in Community Health Informatics, Thailand

Co-organized by:

- Korea Institute of Broadcast and Media Engineers (KIBME), Korea
- Institute of Electronic Information and Communication Engineers (IEICE), Japan
- Institute of Design Information and Electronic Engineers (IDIEE), Japan
- Japanese Society of Precision Engineering (JSPE-GAPE), Japan
- Image Processing and Pattern Recognition Society (IPRS), Taiwan
- IEEE, Taiwan Section

Region of Interest of Human Lumbar Spine Segmentation using Geometric Triangular Analysis

Watcharaphong Yookwan, Krisana Chinnasarn and Benchaporn Jantarakongkul
 Knowledge and Smart Technology Laboratory, Faculty of Informatics,
 Burapha University, Chonburi, Thailand
 w.yookwan@gmail.com, krisana@it.buu.ac.th and jbenchaporn@gmail.com

Abstract— Dual-Energy X-ray Absorptiometry Scanner plays an important role in medical diagnosis and clinical routine. Typically, this kind of machine produces two radiography images of human spine consisted of Anteroposterior and Lateral side. However, these two images provided different viewpoints. In this paper, a method for segmenting region of interest on lumbar spine using a horizontal projection and geometric triangulation analysis is proposed. The proposed method offered an automated detection of lumbar spine that can reduce computational time and complexity in medical diagnosis. The result of the proposed method can help support many applications such as lumbar vertebrae pose segmentation, bone mineral density analysis and vertebral pose deformation.

Keywords—Lateral; Lumbar spine; ROI; Segmentation; Geometric; Triangular Analysis;

I. INTRODUCTION

In diagnosis routine of scoliosis, osteoporosis and osteopenia normally performs by using Bone Mineral Density (BMD) and radiography images which are produced from Dual-Energy X-Ray Absorptiometry scanner or DXA Scanner. DXA produces two radiograph images of human spine consist of Anteroposterior (AP) and right side (Lateral), as shown in Fig 2. The two images provide two different view points. Lateral image shows a whole structure of human spine including Cervical, Thoracic, Lumbar and Sacral. But AP image depicts only the Lumbar region of human spine. Thus, to reduce complexity and computational time, the automatic Region of Interest (ROI) segmentation of lumbar region is an important process in diagnosis and Bone Mineral Density measurement. Including applied method or application such as Lateral lumbar vertebrae pose segmentation or Scoliosis detection and automatic deformation of three-dimensional model of human Lumbar vertebrae.

Most recent research works on lateral lumbar vertebrae segmentation use high resolution X-ray image or CT images. In addition, most of them still manually locate lumbar region. R. Sa et. al. [1] proposed a lateral lumbar vertebrae segmentation in scale-variant high radiant X-ray clinical image.

E. Alvarez Ribeiro et. al. [2] presented a procedure to detect lumbar vertebral in lateral high-dose of X-ray images using Gabor filter. R. Sa et al. [3] demonstrated a method which use R-CNN to detect intervertebral disc in X-Ray image. G. Zheng et al. [4] introduced a method to reconstruct a lumbar vertebral from a single fluoroscopic image. These works use manual method to locate human lumbar spine region before processing.

In this paper, we proposed a new method to automatically segment human lumbar spine region to help support specialist or physician in detecting the boundary of lumbar spine. By using the proposed method, it can automatically detect the lumbar region instead of manually segmenting them. However, the Low-resolution radiograph image is quite difficult to automatically segment.

There are three main steps in the proposed method. Starting from a pre-process using binarization and basic morphological. Next, the horizontal projection profile is used to visualize information of the input image and triangular analysis is used to analyst features. Finally, the region of human lumbar spine region is extracted from original image.

II. BACKGROUND KNOWLEDGE

Recently, medical image analysis is very efficient in many medical or clinical diagnosing routine. Thus, understanding of the core information medical images is needed to process and analyst them. The basic background knowledge is described as below:

A. Lumbar Vertebrae

In human anatomy [5], the five vertebrae pose between the rib cage and the pelvis covered the largest segment of the vertebral column which characterized by the absence of the foramen transversarium within the transverse. They are designated into L1 to L5, from top to bottom. The lumbar vertebrae are the main structure that support the weight of the body and permit movement as shown in .

B. Dual-Energy X-Ray Absorptiometry

Dual-energy x-ray absorptiometry or called in short DEXA, [6] uses a very small dose of ionizing radiation to produce images of the bone structure of the patient who might have a bone disease. It is commonly used to diagnose osteoporosis and to assess an individual's risk for developing

fractures. DEXA is quite a simple machine and noninvasive to both patient and physician. It provides a reasonable accurate method for diagnosing osteoporosis.

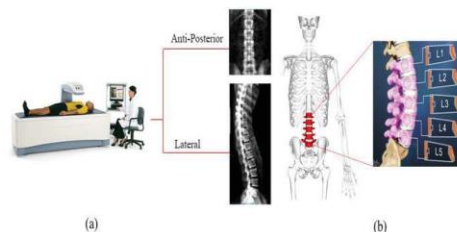


Fig. 1 Dual-Energy X-ray Absorptiometry scanner (a), Lumbar section (b).

C. Morphology Operation

Morphology Operation [7] is a technique for analyzing and processing of geometrical structures which based on set theory, lattice theory, topology, and random functions. It is commonly applied to digital images. However, it can be employed as well on graphs, surface meshes, solids, and many other spatial structures. Morphology technique is used for filling holes and incomplete parts, enlarge areas, and eliminate exceed parts on digital images. In particular, the binary regions produced by simple thresholding may be distorted by noises. In this regard, morphological technique can properly help to remove those noises.

III. METHODOLOGY

In this section, the three steps for identifying the region of interest on human lumbar vertebrae are discussed. They are pre-processing, features selection and then region of interest segmentation.

In this work, the dataset was collected from Burapha university hospital as the input images. The proposed method started from pre-processing process using an entropy value of each image as an initial threshold value for binarization in order to separate background from foreground. Then, morphological operation is applied to remove small objects. Secondly, after insignificant objects were removed, horizontal projection is used to calculate the summation of intensity to plot a time series graph. On this graph, the triangular analysis is applied using law of cosine to identify potential features. Finally, the featured extracted from previous process are used to identify candidate area of interest. Then those candidate areas are used to segment the lumbar spine from radiography image. The framework of proposed method is depicted in Fig. 2

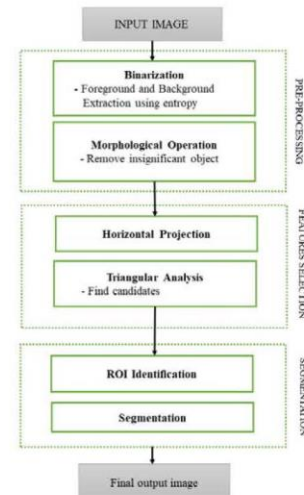


Fig. 2 Overview of proposed method.

A. Pre-processing

Binarization: In this study, Lateral view radiography image produced from DEXA scanner is used as an input image. The binarization process is applied to increase the differentiation between the object of interest and background. In order to make a clear distinction, a technique called “entropy value” proposed by Du-Yih Tsai et. al. [8] is used to measure entropy values of each input image. This value is then set as an initial threshold value to extract foreground from its background. The entropy value is defined by equation (1).

$$E(X) = - \sum_{i=1}^n \sum_{j=1}^m P(x_{ij}) \log_2 P(x_{ij}) \quad (1)$$

Where X is an input image, n is image's width, m is image's height, x_{ij} is intensity in grayscale image and $P(x_{ij})$ is a probability of each x_{ij} .

Morphological Operation: After the binarization process to extract object of interest from background using entropy information, there still be a number of small unconnected objects remained the image. To remove these small objects, the Morphological Opening Operation is employed as defined in equation (2).

$$A \circ B = (A \ominus B) \oplus B \quad (2)$$

Where A is an input image, B is a specific structure element, \ominus is an erosion operation and \oplus is a dilation operation respectively.

Opening Operation is used to remove small objects from the foreground of an image. In this operation, there are two techniques: Erosion and Dilation. Firstly the Erosion technique is used to remove small object in the foreground which may also remove parts of object of interest. Thus, after the Erosion step, the Dilation technique is used to restore the eroded part of object of interest. After applying the opening operation, inconsiderable objects are removed.

B. Features Selection

Horizontal Projection: The output of the pre-processing process as described above, is then projected as a time series graph using horizontal projection. The horizontal projection is a summation of an image's intensity that transform two dimensional information into one dimensional information to reveal pattern of region of interest. The horizontal projection is employed as defined in equation (3).

$$H_k(X) = \sum_{i=1}^n X_{k,i} \quad (3)$$

Where k is an each image's row number, X is an pre-processed input image and n is an image's column number.

The result of horizontal projection can reveal the characteristics of individual parts of the human spine which can later use to determine lumbar section as shown in Fig. 3. That is, the lumbar section can be clearly spotted by an area where the graph obtained lower peaks as compared with the surrounded peaks or look similar like a valley.

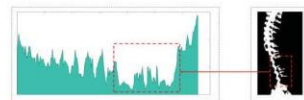


Fig. 3 Horizontal Projection of Lateral X-ray image.

Peaks Finding: In order to identify those peaks, the local maxima information is used to locate each peak. The local maxima is calculated as defined in However, an initial result of local maxima calculation provided too many maxima points or peaks. Therefore, a graph smoothing technique is applied to eliminate those insignificant peaks.

Triangulation: After the local maxima points are identified, the association among peaks are retrieved using triangular shape as shown in Fig. 4. Triangular shape is created using a peak with its left and right adjacent peaks. These triangular shape objects are used to locate the valley area.

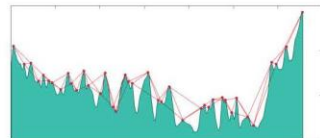


Fig. 4 Triangulate Between Peak Points.

C. Segmentation

Candidates selection: All triangles that generated from peak points in the former step can be classified into 4 patterns: a) left side peak of an examined point is in quadrant two and right side peak is in quadrant one, b) left side peak of an examined point is in quadrant two and right side peak is in quadrant four, c) left side peak of an examined point is in quadrant three and right side peak is in quadrant one and d) left side peak of an examined point is in quadrant three and right side peak is in quadrant four. From those four patterns of triangles, it clearly demonstrated that pattern d) and c) are patterns that corresponding well to the candidate objects. Thus, these patterns are used to determine lumbar section as shown in Fig. 5 (b) and (c).

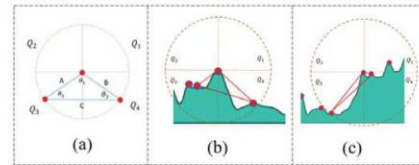


Fig. 5 Example of final candidate triangles.

However, using located quadrant of each triangle is not enough to identify candidate objects. Thus, another feature is needed to help identify them. The proposed method applied interior angle and triangular length to determine candidates. The interior angles are measured using law of cosine [9].

From observation, the boundary of lower lumbar section can be determined by θ_2 . In which, the θ_2 has to be an acute angle, where the value of θ_2 has to be in the range of $0 < \theta_2 < 10$. Furthermore, θ_1 has to be an obtuse angle, where the value of θ_1 has to be in the range of $90 < \theta_1 < 180$ as shown in Fig. 5 (c). Then, triangular length of each object is measured and then compared among all candidate objects to locate the one with maximum value or Length A as shown in Fig. (b). The selected triangle is then used to locate the lower bound of the lumbar section. Likewise, the determination of candidate object for upper lumbar section is identified by θ_3 where θ_3 has to be an acute angle and its value fall into the range of $0 < \theta_3 < 45$. Furthermore, the θ_1 has to be an obtuse angle where θ_1 fall into the range of $90 < \theta_1 < 180$ as shown in Fig. 5 (b). The candidate objects that got the maximum length B is chosen as a selected triangle that used to locate the upper bound of the lumbar section as shown in Fig.6 (d). Algorithm for finding the candidate objects is illustrated in Fig. 7.

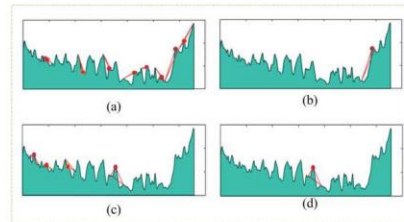


Fig. 6 Finding all possible candidate triangles

Algorithm 1 Candidates Selection

```

Require: Triangles
Ensure: Boundary
1: for  $i = 1 : \text{size}(\text{triangles})$  do
2:    $\text{angles} = \text{anglecalculator}(\text{triangle}(i))$ 
3:    $\text{minangle} = \min(\text{angles}(1))$ 
4:    $n = 1$ 
5:   if  $\text{minangles} \geq 0$  AND  $\text{minangles} \leq 45$  then
6:      $\text{candidates}(n) = \text{triangles}(i)$ 
7:      $n++$ 
8:    $\text{maxdistance} = \min(\text{candidates}(i,2))$ 
9:   for  $i = 1 : \text{size}(\text{candidates})$  do
10:    if  $\text{maxdistance} = \text{candidates}(i,2)$  then
11:       $\text{boundary} = \text{candidates}(i)$ 

```

Fig. 7 Summarize of Candidates Selection Method.

After obtaining information for locating both upper and lower boundary, these information is then used to segment the lumbar region from original input image as shown in Fig. 8.



Fig. 8 Segmented ROI of human lumbar spine region

IV. EXPERIMENTAL RESULT

The dataset used in the lab scale experiment consisted of 50 radiography images of lateral human's spine produced from Dual-Energy X-ray Absorptiometry scanner (DXA Scanner) provided by local hospital. The dataset contains variation of image's quality: high, medium and low quality. These differentiations caused from the volume of radiation exposed to each patient. The higher the volume of radiation used, the better the quality of the image obtained. In the experiment, the automated segmentation of lumbar section was compared with the ground-truth images. The performance evaluation method are Precision and Recall (Confusion Matrix). The experimental result showed that the proposed method gained 81.1% for Accuracy, 90.0% for Precision and 88.5% for Recall.

V. CONCLUSION AND DISCUSSION

In this research, a new method using triangular analysis for lumbar segmentation from low-radiation radiography image produced from Dual-energy X-ray Absorptiometry is proposed. The proposed method consists of three main steps. Firstly, the pre-processing step consists of binarization and morphological techniques. These techniques are applied to remove background and noises. Secondly, the output from step one is transformed into horizontal projection. The output of horizontal projection is then used to find local maxima which located the peak points. Triangular shape is formed using a peak with its left and right adjacent peaks. Finally, candidate objects are determined using the proposed features of the triangular shape. The proposed method can automatically locate the region of human lumbar spine. This can help to reduce work load of radiologist. In general, the proposed method can be used as a preprocess for other research in the area of bone structure identification and segmentation. In future work, the segmentation of lumbar region for special cases of exostosis and bone collapse is going to be attempted.

VI. ACKNOWLEDGEMENT

This work was financially supported by the Research Grant of Burapha University through the National Research Council of Thailand (NRCT), fiscal year 2018 and Faculty of Informatics, Burapha University.

VII. REFERENCES

- [1] R. Sa, W. Owens, R. Wiegand and V. Chaudhary, "Fast scale-invariant lateral lumbar vertebrae detection and segmentation in X-ray images," *2016 38th Annual International Conference of the IEEE Engineering in Medicine and Biology Society (EMBC)*, Orlando, FL, 2016, pp. 1054-1057.
- [2] E. Alvarez Ribeiro, M. H. Nogueira-Barbosa, R. M. Rangayyan and P. M. Azevedo-Marques, "Detection of vertebral plateaus in lateral lumbar spinal X-ray images with Gabor filters," *2010 Annual International Conference of the IEEE Engineering in Medicine and Biology, Buenos Aires*, 2010, pp. 4052-4055.
- [3] R. Sa et al., "Intervertebral disc detection in X-ray images using faster R-CNN," *2017 39th Annual International Conference of the IEEE Engineering in Medicine and Biology Society (EMBC)*, Seogwipo, 2017, pp. 564-567.
- [4] G. Zheng, L. P. Nolte and S. J. Ferguson, "2D/3D reconstruction of a scaled lumbar vertebral model from a single fluoroscopic image," *2010 Annual International Conference of the IEEE Engineering in Medicine and Biology*, Buenos Aires, 2010, pp. 4395-4398.
- [5] Lumbar vertebrae. (2017, October 26). In Wikipedia, *The Free Encyclopedia*. Retrieved 17:33, October 26, 2017, from <https://goo.gl/M14wtbDual-energy X-ray absorptiometry>. (2017, September 14). In Wikipedia, *The Free Encyclopedia*. Retrieved 17:31, October 26, 2017, from <https://en.wikipedia.org>
- [6] [g/w/index.php?title=Dual-energy X-ray absorptiometry&oldid=800563432](https://en.wikipedia.org/wiki/Dual-energy_X-ray_absorptiometry)
- [7] Mathematical morphology. (2017, July 8). In Wikipedia, *The Free Encyclopedia*. Retrieved 16:44, October 31, 2017, from https://en.wikipedia.org/w/index.php?title=Mathematical_morphology&oldid=789586533
- [8] Tsai, D.Y., Lee, Y. & Matsuyama, E. *J Digit Imaging* (2008) 21: 338.
- [9] Law of cosines. (2017, October 18). In Wikipedia, *The Free Encyclopedia*. Retrieved 07:51, November 4, 2017, from https://en.wikipedia.org/w/index.php?title=Law_of_cosines&oldid=805979763





ICAICTA 2018
International Conference on Advanced Informatics:
Concepts, Theory and Applications
Conference : 14-17 August, 2018 | Krabi, Thailand

ICAICTA 2018

@Krabi, Thailand

August 14 - 17, 2018

Call for Papers

ICAICTA 2018 - International Conference on Advanced Informatics: Concept Theory and Applications

Prospective authors are invited to submit full papers of no more than six (6) pages including results, according to template provided below. Papers will be subject to double blind peer review in which the reviewers do not know the author's identity. In order to make blind reviewing possible, authors must omit their names and affiliations from the paper.

Conference website : <http://services.informatics.buu.ac.th/icaicta2018/>

Scope of Conference

Computational Science and Engineering
High Performance Computing
Distributed Systems and Pervasive Computing
Numerical Methods and Simulations
Game Theory and Optimizations
Cryptography and Data Hiding

Media Technology and Information Systems
Computer Vision, Graphics, and Image Processing
Natural Language and Speech Processing
Human Computer Interactions
Multimedia Services and Applications
Audit, Security and Governance
Intelligent Robotics

Intelligent Systems and Data Sciences
Information Retrieval and Data Mining
Database and Programming
Artificial Intelligence and Machine Learning
Expert and Recommendation Systems
Learning Systems and Knowledge Modeling

Computation for Science
Computational Chemistry
Computational Physics
Computational Biology
Computational Social Science



Timeline of key dates:

- Dec 1, 2017: CALL FOR PAPERS
- June 15, 2018 (EXTENDED): SUBMISSION DEADLINE
- Jul 10, 2018: NOTIFICATION OF ACCEPTANCE
- Jul 15, 2018: EARLY-BIRD REGISTRATION
- Jul 25, 2018: CAMERA-READY SUBMISSION
- Aug 1, 2018: REGULAR REGISTRATION
- Aug 14 - 17, 2018: CONFERENCE DAY



Logos of partner institutions and IEEE:

- TOYOHASHI UNIVERSITY OF ECONOMICS
- UNIVERSITY OF TECHNOLOGY (UT)
- UNIVERSITI SAINS MALAYSIA (USM)
- BUENAVISTA UNIVERSITY
- IEEE
- IEEE Xplore Digital Library
- IEEE THAILAND SECTION

Automated Vertebrae Pose Estimation in Low-Radiation Image using Modified Gabor Filter and Ellipse Analysis

Watcharaphong Yookwan¹, Krisana Chinnasarn² and Benchaporn Jantarakongkul³
 Faculty of Informatics, Burapha University, Thailand
 w.yookwan@gmail.com¹, krisana@it.buu.ac.th² and jbenchaporn@gmail.com³

Abstract— Dual-Energy X-ray Absorptiometry Scanner plays an important role in medical diagnosis and clinical routine. Typically, this kind of machine produces two radiography images of human spine consisted of Anteroposterior and Lateral side. However, these two images provided different viewpoints. This paper proposed a method to automatically estimate human vertebrae pose in lateral-side image by using Multi-theta Orientation Gabor Filter combined with Principle Component Analysis and Geometric Ellipse Shape Analysis. The proposed method offered an automated estimation of human lumbar vertebrae pose that can reduce work load of radiologist, computational time and complexity in various bone-clinical applications. The result of the proposed method can help support many applications such as lumbar vertebrae pose segmentation, bone mineral density analysis and vertebral pose deformation. The proposed method can estimate the vertebrae pose with 86.4% for accuracy, 80.5% of recall, precision for 89.11% and 13.6% of false negative rate.

Keywords; vertebrae pose segmentation; Gabor filter; Ellipse-shape; PCA; Multi-theta; lateral;

I. INTRODUCTION

There are some diseases which occurred on human Lumbar Spine such as Scoliosis, Bone Collapse and Degenerative Disc Disease (DDD). These kinds of diseases need to be followed up regularly [1]. Thus, patients are unavoidable to expose to X-Radiation. However, continuous treatment may lead to over limit radioactive absorption per calendar year (0.05 Sv per year) [2]. Hence, low-radiation scanner like Dual-energy X-ray Absorptiometry or DXA scanner is often used to avoid over dose radiation [3]. DXA Scanner radiates a very small dose, 1-4 uSv (0.00001 Sv–0.00004 Sv) or 8 hours more expose to radioactive, compare to natural radiation (8 uSv per day) [4]. Nevertheless, images produced from low-radiation scanner provided low quality images which difficult to detect and identify vertebrae pose.

Many recent studies proposed a variety of methodologies for vertebrae segmentation on Magnetic Resonance Imaging (MRI) images. S. Ghosh et al. proposed a new approach to automate disc localization in clinical lumbar from MRI image

using machine learning with heuristics [5]. This research used Histogram of Oriented Gradients (HOG) together with Support Vector Machine (SVM) as classifier. The experimental results achieved an accuracy rate of 99% for disc localization on 53 clinical cases (318 lumbar discs). Y. J. Zhao et al. presented a method to segment a vertebrae pose using shape of vertebrae spine segment extracted using improved GVF snake [6]. This research proposed a semi-automatic segmentation method in which 12-points (12-anatomical point representation) was manually annotated on the region of interest (ROI) before the ROI on target object can be extracted automatically. C. S. Ling et al. introduced semi-automated vertebral segmentation of human spine on MRI images [7].

Not only MRI images are used to segment lumbar vertebrae segmentation but also Computational Thermography images were widely used. J. Patrick and M. G. Indu proposed a semi-automated method to segment vertebrae on CT images [8]. The vertebral body is identified using iterative Normalized-cut algorithm for detection process which applied eigenvalue decomposition. For segmentation technique, region based active contour method was proposed to segment individual vertebrae. Y. Li et al. proposed an automatic initialized level set approach based on region correlation for lumbar vertebrae segmentation on CT image [9]. S. Kadoury et al. presented a spine segmentation using Manifold Embeddings and Higher-Order MRFs [10].

Even though, the proposed method mentioned above can offer good results. But MRI and CT techniques which provided good quality images (low noise with high contrast) are often used for non-regular treatments. Therefore, for those patients that need follow up treatments might be at risk of over dose exposure to radiation. In this paper, a new vertebrae pose estimation from lateral side method is proposed. The proposed method is divided into three main phases. In the first phase, Top-hat filtering is applied to enhance an input image. In the second phase, Multi-theta Orientation Gabor filter is performed to segment vertebrae pose object. In this phase, those small objects are also removed. In the last phase, all connected components are labelled before Principle Component Analysis (PCA) is

applied to create an ellipse-shape. Object with non-ellipse shape will be removed. Finally, vertebrae pose is estimated using a major axis of ellipse.

II. BACKGROUND KNOWLEDGE

A. Dual-Energy X-ray Absorptionmetry : DXA Scanner

Dual Energy X-ray Absorptionmetry is a machine that used in bone scanning and bone mineral density measurement. DEXA scanner produces two levels of radiation energy. One is low level of energy and other is high level of energy [11]. Thus, Patients will expose a very low radiation (only 1-4 uSv (0.00001 Sv-0.00004 Sv)

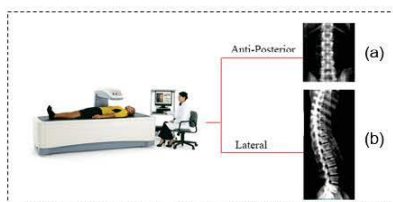


Fig 1 Radiography images produced from DXA Scanner. Consist of 2 images, Anti-Posterior (a) and Lateral (b)

B. Top-Hat Filtering

Top-hat filtering is used in image contrast enhancement using morphological operation [12]. It removes small object with darker image by subtracting original image with opened image as defined in Eq. 1. First, start with image erosion (Eq.3) for object size reduction, then dilate the image (Eq.4) to increase the object size and small object removing.

$$I_{TH} = I - (I \circ S) \quad (1)$$

Let I_{TH} is an image with top-hat filtered, I is an original image, S is a disk-shaped structure element and $I \circ S$ is an opened image by structure element. The opening operation can be described as Eq. 2

$$I \circ S = (I \ominus S) \oplus S \quad (2)$$

Let $I \ominus S$ and $I \oplus S$ is an eroded image and dilated image respectively. Image erosion and image dilation can be defined in Eq.3 and Eq.4

$$I \ominus S = \min_{u,v} \{I_{x+u,y+v} - S_{u,v}\} \quad (3)$$

$$I \oplus S = \max_{u,v} \{I_{x+u,y+v} - S_{u,v}\} \quad (4)$$

Let x,y is a coordinates of an original image and u,v is a coordinates of disk-shaped structure element.

C. Gabor Filtering

Gabor filtering is usually used in analysis texture. It means that, it normally used to analyst image's content or pattern in frequency specifically and specific direction. So that, Gabor filtering can detect any objects in each given directions. Many researcher claims that Gabor filtering is similar to human vision [13]. Gabor filters have been used in

many applications, such as segmentation of texture, identification of target object, analysis of some type of document, dimension management fractal, detecting edge in images, image representation and identity determination. By using Gaussian and Sine wave, allow us to extract objects in image with specific orientation [14].

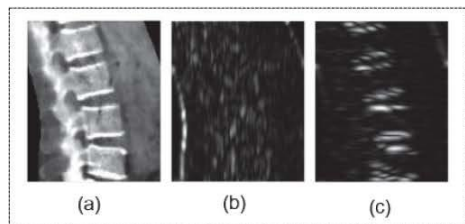


Fig 2 Example of applying Gabor filter to original grayscale image(a), output of Gabor filtering with $\theta = 0$ (b) and output of Gabor filter with $\theta = 90$ (c)

A variety of different orientation and frequency is very useful to extract an important object from an original image. In the uncontinuous domain, two-dimensional Gabor filters are given by,

$$I_{gb}(\theta) = \sum_u \sum_v (I_{x-u,y-v}) G_{u,v}(\theta) \quad (5)$$

Let I_{gb} is a Gabor filtered image, $I_{x-u,y-v}$ is an original image and $G_{u,v}$ is a Gabor filter with size of $u \times v$. Gabor filter can be described in Eq. 6 below.

$$G_{x,y}(\theta) = e^{\left\{ \frac{1}{2} \left(\frac{x^2}{\sigma_x^2} + \frac{y^2}{\sigma_y^2} \right) \right\}} \cos(2\pi f x) \quad (6)$$

x and y Can be defined as:

$$x = x \cos \theta + y \sin \theta \quad (7)$$

$$y = -x \sin \theta + y \cos \theta \quad (8)$$

Where f is a modulation of frequencies, σ_x is a Gaussian boundary in x axis and σ_y is a Gaussian boundary in y axis.

D. Principle Component Analysis (PCA)

Principal component analysis or PCA is a method in statistical. It converts a set of interested of possibly correlated variables in to a linearly variable without correlation (Principal Component by using an orthogonal transformation [14]. Principal Component Analysis is used to transform data in to a new system of coordinating and defined as linear orthogonal

transformation. The largest variance value of data is called the first component. The smaller variance value is called second component.

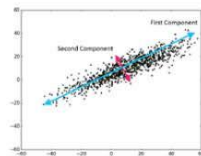


Fig 3 First Component and Second Component Analysis

E. Connected-Component labelling

Connected-Component Labelling is a method to label or identify the unique object by using graph theory and given heuristic function. Connected-Component Labelling is commonly used in image processing. By using kernel (Structure Element as shown in Fig. 4.), it can identify the connected object or regions in an image. It can be done in two passed operation. First pass is to make a temporary label and equivalent. The second pass is to change each temporary label with the smallest value of its equivalent label

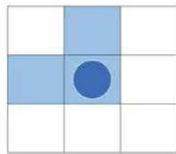


Fig 4 Structure Element for Connected-Component Labelling

F. Geometric Ellipse Shape

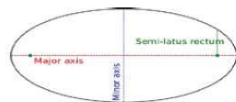


Fig 5 Properties of ellipse shape

Ellipse is a planar curve which in some Cartesian system of coordinates is described by the Eq. 9 below:

$$\frac{x^2}{a^2} + \frac{y^2}{b^2} = 1; a, b > 0 \quad (9)$$

Where x and y is coordinate point, a and b is a major axis and minor axis length respectively. A region of ellipse can be computed from

$$\frac{(x-x_c)^2}{a^2} + \frac{(y-y_c)^2}{b^2} = 1; a, b > 0 \quad (10)$$

Where x_c is the center along x -axis and y_c is the center along y -axis.

III. METHODOLGY

In this section, the proposed method to estimate vertebrae pose in low radiation image is briefly demonstrated in Fig. 6. The

approach start from enhancing an input image using Top-Hat filtering. Then, Multi-theta orientation Gabor filter is employed to extract objects in each specific orientations. After that, insignificantly small objects are removed. Secondly, Geometric Ellipse-shape is created using Principle Component Analysis to determine the vertebrae poses area and each oriaintations. Finally, the vertebrae poses are identified.

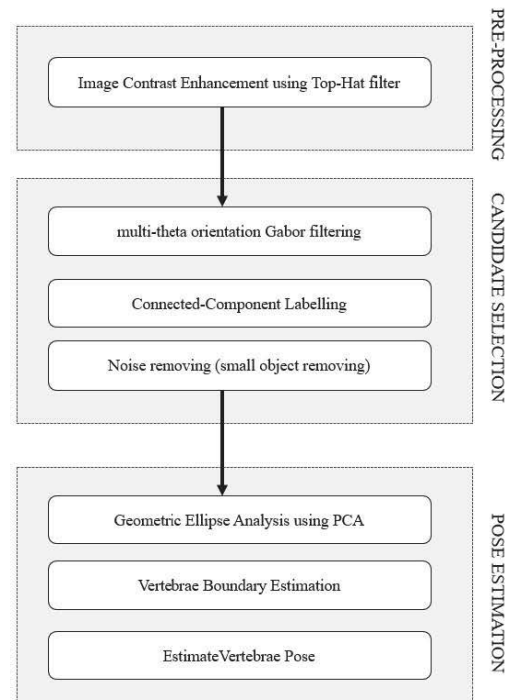


Fig 6 Proposed method

A. Image Contrast Enhancement using Top-Hat Filter

According to Eq.1. Since the opening operator leaves a background of the image, it is expected that Top-Hat filter removes the image background. This filter acts like a high-pass filter and extracts the bright areas then remove dark areas of the image as shown in an output image result in Fig. 6 (b)

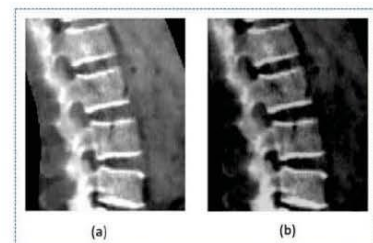


Fig 7 Original grayscale image (a), output of Top-hat filtered image (b)

B. Multi-theta Orientation gabor filter

As shown in Eq.5 and Eq.6 Gabor filter is used to extract an object in specific orientation degree. Nevertheless, the interested object (Vertebrae posed) in this dataset appears in variety of orientation degree. Thus, Multi-theta Orientation Gabor filter is employed to extracted object in variety of degrees.

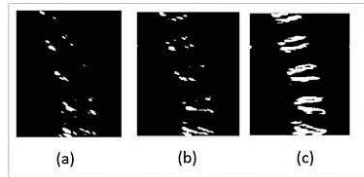


Fig 8 Output binary image from Gabor filter with $\theta = 60$ (a), $\theta = 90$ (b) and Binary output from Multi-theta orientation Gabor filter (c)

As shown in Fig.8 (a) and Fig.8 (b), output image of Gabor filter with $\theta = 60$ and $\theta = 90$ reveals only few parts of interested objects. So that, Output images of Gabor filter in range of $\theta = 60$ and $\theta = 120$ are merged into one output image as demonstrate in Fig. 7 (c) and can be defined as Eq. 11

$$I_{mgb}(\theta_1, \theta_2) = \sum_{i=\theta_1}^{\theta_2-1} \{ I_{gb}(i) \cup I_{gb}(i+1) \} \quad (11)$$

Let I_{mgb} is an output image of Multi-theta Orientation Gabor filter. θ_1, θ_2 are the initial and final theta of Gabor filter function respectively and I_{gb} is an output of Gabor filter function as described in Eq. 5

```

Algorithm Gabor Filtering
Require : sigma, theta, lambda, psi, gamma
Ensure : gb (Gabor Filter)
1: sigma_x = sigma
2: sigma_y = sigma/gamma
3: nstds = 3
4: xmax = max(abs(nstds*sigma_x*cos(theta)),
              abs(nstds*sigma_y*sin(theta)))
5: xmax = ceil(max(1, xmax))
6: ymax = max(abs(nstds*sigma_x*sin(theta)),
              abs(nstds*sigma_y*cos(theta)))
7: ymax = ceil(max(1, ymax))
8: xmin = -xmax; ymin = -ymax
9: [x, y] = meshgrid(xmin:xmax, ymin:ymax)
10: x_theta = x*cos(theta)+y*sin(theta)
11: y_theta = -x*sin(theta)+y*cos(theta)

```

Fig 9 Algorithm of Gabor Filtering

```

Algorithm Multi-theta orientation Gabor Filtering
Require : initTheta, stopTheta, step, img
Ensure : output_img
1: For i = initTheta : step : stopTheta
2:   Bw = gabor_filter(img, i)
3:   output_img = merge(output_img, Bw)
4: endfor

```

Fig 10 Algorithm of Multi-theta Gabor Filtering

C. Noise Removing

In this step, opening image morphology is used to remove insignificantly small objects in the binary output image from

multi-theta orientation Gabor filter. Opening image morphological can be described in Eq.2. The output of noise removing using opening image morphological is shown below in Fig. 11

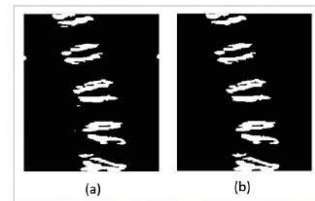


Fig 11 Output of multi-theta orientation Gabor filter (a) and output of opening image morphological (b)

D. Connected-Component Labelling

After obtained binary image from previous process, the objects in the image are labelled as shown in Fig.10 (b) Connected-component can be labelled by using a structure element as demonstrate in Fig. 12



Fig 12 Labeled objects in Multi-theta orientation Gabor filter image

E. Geometric-Ellipse Analysis

Shape of human lumbar vertebrae pose looks similar to ellipse shape as shown in Fig. 13

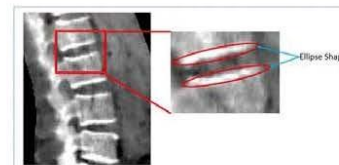


Fig 13 Ellipse-Shape like of human vertebrae pose

After removed small objects, Geometric Ellipse is applied to analyze the shape of vertebrae pose. Once the objects in the image are labelled, ellipse shape objects are generated using a point in center of each objects as a center point of each one ellipse. The proposed method used ellipse analysis to differentiate among different patterns of bone structure. The ellipse equation is calculated from Eq.9 By using Principle Component Analysis (PCA), the major axis, minor axis and orientation of each objects are calculated. The first component and the second component of each objects are become an Ellipse major axis and minor axis respectively as demonstrated in Fig.13

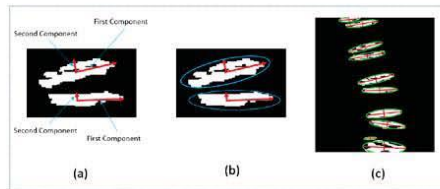


Fig 14 The first and second component of each objects (a), Apply an ellipse shape using the first and the second components (b), all ellipse with major axis and minor axis.

After represented all objects in binary image by Ellipse shape from PCA. The ellipse which length of major axis long $\frac{3}{4}$ or more than the average of all ellipse are selected as a candidates for identifying a vertebrae pose.

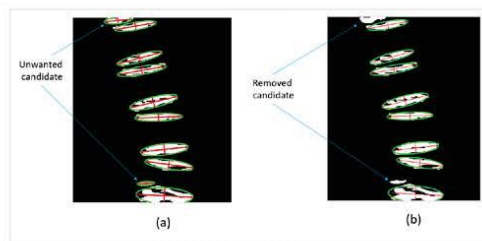


Fig 15 All candidates (a), selected candidates (b)

After selected candidates, the left and right boundary of each vertebrae pose are estimated using polynomial with degree of three are employed as shown in Fig.15 (a). Curve fitting can be defined as below:

$$P(x) = P_1x^n + P_2x^{n-1} + \dots + P_nx^n + P_{n+1} \quad (12)$$

$$y = P_1x^n + P_2x^{n-1} + \dots + P_nx^n + P_{n+1} \quad (13)$$

Where $P(x)$ is the coefficient, y is the value of a polynomial, n is the degree of polynomial. In this research, a degree is equal to 3. This is because the spine structure have a curved like shape. The coordinates of each ellipse's major axis right and left are used to fit the curve. Then, vertebrae pose are estimated as shown in Fig. 16 (c)

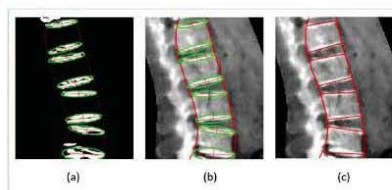


Fig 16 Selected candidates and vertebrae boundary estimation using curve fitting in binary image (a), Selected candidates and vertebrae boundary estimation using curve fitting in grayscale image (b), final output of vertebrae pose estimation (c)

IV. EXPERIMENTAL RESULT

In the proposed method, the dataset which contained 100 low radiation lateral-side lumbar vertebrae images were collected from local hospital. The images produced from Dual-Energy X-ray Absorptiometry (DEXA) consist of low quality, medium quality and high quality image. The experimental result is compared with ground-truth which provided by experts radiologist from local hospital. The efficient was evaluated by using confusion matrix. The result is shown in Table. I

TABLE I EFFICIENCY OF THE PROPOSED METHOD

Accuracy	Recall	Precision	False Negative rate
86.4%	80.5%	89.11%	13.6%


V. CONCLUSION AND DISCUSSION

This research proposed the method to automatically estimate vertebrae pose in low-radiation X-ray image. The datasets were produced from Dual-Energy X-ray Absorptiometry (DEXA) from local hospital. By using Modified Gabor filter combining with geometric ellipse shape analysis, the vertebrae pose is estimated. The proposed method is divided in 3 main phases. In the first phase, the input image is enhanced using Top-Hat filtering. In the second phase, multi-theta orientation Gabor filter is used to extract vertebrae pose candidates. Then, all connected-component candidates are labeled for removing all small candidates. In the final phase, Principle Component Analysis (PCA) and Ellipsoidal Analysis are used to determine orientation of each vertebrae pose. After that, lumbar spine line is estimated using polynomial curve fitting. The proposed method can automatically estimate the region of human lumbar vertebrae pose with 86.4% of accuracy, 89.11% of precision 80.5% of recall and 13.6% of false negative rate. This can help to reduce work load of radiologist. The proposed method can be used as a pre-process for many other researches such as bone structure identification and segmentation, bone lesion identification, and also in three-dimensional bone reconstruction. However, the proposed method cannot work in the dataset with high-level damaged vertebrae pose from lesion of exostosis and bone collapse. In future work, the identification of lumbar vertebrae pose for special cases of exostosis and bone collapse is going to be attempted.

ACKNOWLEDGMENT

This work was financially supported by the Research Grant of Burapha University through the National Research Council of Thailand (NRCT), fiscal year 2018 and Faculty of Informatics, Burapha University.

REFERENCES

- 
- [1] Calenbergh, F.V., Casey, A.T., Goffin, J., Kehr, P., Loon, J.P., Liebig, K., Lind, B., Logroscino, C.A., Pointillart, V., & Sgrambiglia, R. (2003). Intermediate follow-up after treatment of degenerative disc disease with the Bryan Cervical Disc Prosthesis: single-level and bi-level. *Spine*, 28 24, 2673-8.J.
- [2] Occupational Radiation Exposure Limits. (n.d.). Retrieved March 27, 2018, from http://ursa.research.gsu.edu/radiation-safety/occupational-radiation-exposure-limits/K_Elissa. "Title of paper if known," unpublished.
- [3] Wikipedia contributors. (2018, February 16). Dual-energy X-ray absorptiometry. In Wikipedia, The Free Encyclopedia. Retrieved 04:12, March 27, 2018, from https://en.wikipedia.org/w/index.php?title=Dual-energy_X-ray_absorptiometry&oldid=825987773.
- [4] Levitt, L. (2017, July 04). DEXA scans & Radiation. Retrieved March 27, 2018, from <http://www.measureup.com.au/dexa-scans-radiation/>.
- [5] S. Ghosh, M. R. Malgireddy, V. Chaudhary and G. Dhillon, "A new approach to automatic disc localization in clinical lumbar MRI: Combining machine learning with heuristics," 2012 9th IEEE International Symposium on Biomedical Imaging (ISBI), Barcelona, 2012, pp. 114-117.
- [6] Y. J. Zhao, L. Shi, J. C. Li, J. F. Griffith, A. T. Ahuja and P. A. Heng, "Vertebra segmentation of spine MRI with improved GVF snake based on shape knowledge," 2011 International Conference on Machine Learning and Cybernetics, Guilin, 2011, pp. 1867-1871
- [7] C. S. Ling, W. M. Diyana, W. Zaki, A. Hussain and H. A. Hamid, "Semi-automated vertebral segmentation of human spine in MRI images," 2016 International Conference on Advances in Electrical, Electronic and Systems Engineering (ICAEES), Putrajaya, 2016, pp. 120-124.
- [8] J. Patrick and M. G. Indu, "A semi-automated technique for vertebrae detection and segmentation from CT images of spine," 2016 International Conference on Communication Systems and Networks (ComNet), Thiruvananthapuram, 2016, pp. 44-49.
- [9] Y. Li, W. Liang, J. Tan and Y. Zhang, "A novel automatically initialized level set approach based on region correlation for lumbar vertebrae CT image segmentation," 2015 IEEE International Symposium on Medical Measurements and Applications (MeMeA) Proceedings, Turin, 2015, pp. 291-296.
- [10] S. Kadoury, H. Labelle and N. Paragios, "Spine Segmentation in Medical Images Using Manifold Embeddings and Higher-Order MRFs," in *IEEE Transactions on Medical Imaging*, vol. 32, no. 7, pp. 1227-1238, July 2013
- [11] Definition of DXA. (n.d.). Retrieved March 29, 2018, from <https://www.medicinenet.com/script/main/art.asp?articlekey=24486>
- [12] Hamid Hassanpour, Najmeh Samadiani, S.M. Mahdi Salehi, Using morphological transforms to enhance the contrast of medical images, *The Egyptian Journal of Radiology and Nuclear Medicine*, Volume 46, Issue 2, 2015, Pages 481-489, ISSN 0378-603X
- [13] (n.d.). Retrieved March 29, 2018, from http://homepages.inf.ed.ac.uk/rbf/CVonline/LOCAL_COPIES/TRAPPI/filter.html
- [14] (n.d.). Retrieved March 29, 2018, from <https://www.cs.utah.edu/~arul/report/node13.html>
- [15] Wikipedia contributors. (2018, March 22). Connected-component labeling. In Wikipedia, The Free Encyclopedia. Retrieved 08:02, March 29, 2018, from https://en.wikipedia.org/w/index.php?title=Connected-component_labeling&oldid=831792241
- [16] PCA
- [17] Wikipedia contributors. (2018, January 19). Curve fitting. In Wikipedia, The Free Encyclopedia. Retrieved 08:26, March 29, 2018, from https://en.wikipedia.org/w/index.php?title=Curve_fitting&oldid=821310968



REFERENCES



BIOGRAPHY

NAME Watcharaphong Yookwan

DATE OF BIRTH 4 October 1993

PLACE OF BIRTH Bangkok

PRESENT ADDRESS 58/3 Banlane Bangpa-in Ayutthaya 13160

POSITION HELD Student

EDUCATION Bachelor of Science Program in Computer Science

